PLANNING RESILIENT INFRASTRUCTURE

A Dissertation

Presented to the Faculty of the Graduate School

of Cornell University

In Partial Fulfillment of the Requirements for the Degree of

Doctor of Philosophy

by

Arash Beheshtian

August 2016

PLANNING RESILIENT INFRASTRUCTURE

Arash Beheshtian, Ph. D.

Cornell University 2016

The arrival of three extreme weather episodes in a period of fourteen months, each with the odds of a 100-year occurrence suggest that extreme weathers are 'the new normal' in the State of New York. Such intensive and frequent extreme events have induced New York City and also State policy-makers to investigate and possibly develop a set of robust, less vulnerable, and resilience-enhanced critical infrastructures.

Following such recognition and while a majority of resilience-enhancing reports fail to address analytical aspects of the interdependent critical infrastructures, we took on this challenge and investigated 'a planning response' to explore policy options for guiding where to build, what to build, and how to strengthen transportation fueling infrastructure efficiently.

By interfacing qualitative and quantitative paradigms, the proposed models illustrate how to allocate resources proactively and how the network's absorptive, adaptive, and restorative capacities could be together enhanced towards the system's optimum resilience. Results also emphasize on the importance of an integrated planning approach where higher degree of resilience aligned with less costly resilience-enhancing strategies is expected through smart-allocation of resources across the network's elements.

Knowledge of these patterns provides an important basis for evaluating and improving decisions to reduce and otherwise manage infrastructures' vulnerabilities, and could be used as a decision-making tool for assisting planners to better understand and implement esilience-enhancing strategies.

BIOGRAPHICAL SKETCH

Arash Beheshtian was born in Tehran, Iran. He studied Civil Engineering, Urban and Regional Planning, Transportation Engineering, and Transportation Systems Engineering, and worked as an engineer from 2002 to 2009. In the Fall of 2012 he joined Cornell University to pursue his doctoral studies and since then, his research was focused on resilience planning for the critical infrastructures.

To my parents for their endless love and support

ACKNOWLEDGMENTS

I would like to express the deepest appreciation to my committee chair, Professor Kieran P. Donaghy for his extensive support, who has the attitude and the substance of a genius: he continually and convincingly conveyed a spirit of adventure in regard to research and scholarship, and an excitement in regard to teaching. Without his guidance, inspiration, courage, and persistent help this dissertation would not have been possible.

I would like to thank my committee members, Professor Mark A. Turnquist, Professor Linda K. Nozick, and Professor Huaizhu (Oliver) Gao for all their supports. In addition, I want to acknowledge a special debt to Professor Omid M. Rouhani, a true friend, for his close collaboration and help in every step of this work.

TABLE OF CONTENTS

LIST OF FIGURES

LIST OF TABLES

CHAPTER 1

VULNERABILITY ANALYSIS OF NEW YORK CITY'S MOTOR FUEL SUPPLY CHAIN NETWORK

1.1. Introduction

Among metropolitan infrastructures, transportation networks and infrastructures such as motor fuel supply-chain (FSC), functioning interdependently with transportation networks are critical, affecting a metropolitan area's performance and playing crucial role in regional and national wellbeing. Despite the vitality of operable metropolitan infrastructures, keeping these critical networks functional is a complex task, in particular when the arrival of extreme weather episodes has become a 'new normal.' This complexity, however, is multifold and driven by a number of causes. First, urban infrastructures are complex by nature. In addition to dynamic behavior and existing interdependencies across interlinked infrastructures, the large size makes metropolitan infrastructures complex to design and operate. Second, a majority of urban America's infrastructures are nearing the end of their service lives.

Aging, and in many cases over-capacitated infrastructures, introduce a new class of operational difficulty. Third, urban infrastructures are vulnerable to sudden extreme events. Indirect failures ripple from interdependent networks and direct-exogenous shocks imposed by extreme events such as terrorist attacks or severe weather episodes causing different levels of disruption or even failures across the networks' elements.

Within the framework of vulnerability analysis of metropolitan physical networks, a large number of modeling techniques, analytical tools, and quantitative approaches has been developed to address infrastructures' inoperability in time of disasters. Through such effort, technical terms such as criticality (*30*)-(*31*), robustness (*28*)-(*29*), connectivity (*33*)-(*34*), reliability (*35*), susceptibility (*36*), adoptability (*32*), availability (*37*), and resiliency (*1*) are defined. Corresponding modeling approaches have been developed within the context of operation research and systems engineering to address infrastructures' performance while under attack or stress.

The most common method to perform these quantitative techniques is through i) simulating a shock, whether exogenous or endogenous, ii) imposing the simulated shock on network element(s), and iii) assessing network performance under one such disruption. In spite of the fundamental difference in the last step, all network disruption analysis (NDA) approaches adopt the same concept to simulate and impose the arrival of shock. By relaxing one or more network elements and assessing infrastructure's functionality, NDA techniques identify and rank the most critical network element(s) with respect to the infrastructure functionality index. The network element(s) relaxation generally takes place under three lines of methods: single-link failure, multi-link failures, and grid-based approach.

In either of these methods, two strong assumptions are made. First, all elements of the physical infrastructure are fully operable, except the relaxed element(s). Second, there is no interdependency across the network of interest and other infrastructures. The former assumption might be held valid, if the simulated shock and its magnitude of sprawl is limited and known—such as terrorist attacks or other man-made hazards. However, in case of natural disasters, network disruption is not confined to a limited number of elements and typically affects a wider geographical area.

For instance, in case of the super-storm Sandy, 51 square miles of New York City (NYC) flooded— 17 percent of the City's total land mass. Even though the flooded area was less than one-fifth of the City's total area, critical infrastructures such as transportation, transit, and motor fuel supply-chains were fully inoperable for several days following the storm's arrival and did not entirely recovered for months.

The latter assumption also is not factual due to inevitable interdependencies across critical infrastructures.[1] Any given network which is geographically located in non-vulnerable areas may possibly experience inoperability because of cascading failure(s) rippling across other critical networks. Transportation and its corresponding energy/fueling networks are examples of sets of infrastructures having strong interconnectedness. Performance of one depends on the operability and productiveness of the other, and

[1] Interdependencies vary widely and can be divided into different classes such as proximal, cyber, functional, physical, financial, or even logical.

shocks can be transferred due to interdependencies between components. Such ripple effects can also be the source of 'cascading failures,' that is, the failure of a particular system can be the source of failure of another system. Simple examples may be used to illustrate the notion of transition and its relation to interdependency—failure of an electricity grid may stop a subway system from functioning causing transportation modal shift from transit to private vehicle. Drivers mired in the ensuing traffic jam and gasoline delivery trucks stuck *en route* (since they share the same distribution network with private vehicles) eventually contribute to the failure of the fueling network. This is reinforced by the limited number of fueling trucks being able to cope with the escalating rate of gasoline demand.

During and post-Sandy, for instance, a number of the City's physical networks faced major interruptions. In particular, the City's FSC faced extensive and broad disruptions, refineries and terminals lost power and were damaged, and pipelines shut down; all of which led to the widespread gas station closures. Contrary to the popular conclusion that these closures were due to power outages preventing stations from pumping gas, the larger problem turned out to be that stations simply had no gas to pump. According to the U.S. Energy Information Administration (EIA), from the days of the 4th through the11th following Sandy, 67-28 percent of gas stations across the New York metropolitan area (and larger ratio in the City of Manhattan) did not have gasoline available for sale.

The reason behind the post-Sandy supply deficit related to the inoperability of almost every element in the fueling infrastructure. In addition to a total of 28 terminals affected by Sandy, thousands of roads were closed because of downed power lines or tree limbs hampering the ability of trucks to get to open terminals or deliver fuel, even if they were able to obtain it. The station closures, along with the long lines at the stations having gas available, not only limited mobility and slowed economic activity, it also hampered recovery efforts causing cascading failures across other critical infrastructures like transportation and transit networks.

In this paper, we develop the concept of 'vulnerability analysis' within the context of 'supply-chain management' and study Manhattan's motor fuel supply-chain vulnerability in the face of severe weather

episodes. To this end, we relax earlier discussed assumptions and advance a methodology of a vulnerability assessment of spatially dispersed critical infrastructure networks in the face of extreme weather episodes and then examine the proposed method for the case of Manhattan's FSC.

Through the following sections, we develop a mathematical program. The proposed model is structured within the concept of asset allocation optimization methodology. The uncertainty in arrival of extreme events combined with the separation of pre-event investments and post-event network performance lead the proposed mathematical program to a stochastic bi-stage format where fuel replenishment/distribution task (second stage variables) is conditioned on the resource investment decision made within the first stage. The key objective of the proposed model is to investigate an optimum asset allocation strategy which provides the FSC with maximum robustness (i.e. less vulnerability) in the face of extreme weather episodes.

1.2. Literature Review

Herein, we review literatures in two categories of shock simulation and vulnerability assessment analysis.

1.2.1. Shock Simulation Techniques

1.2.1.1.Element-based Vulnerability Analysis[2]

A common approach for the shock simulation techniques in scenario-specific studies is based on the failure of the network's arc(s), whether through single-link failure or multiple-link failures (*20*)-(*22*). The non-deterministic properties corresponding to the shock imposition such as the occurrence chance, randomized location, and intensity happen through several methods such as Semi-Markov Chain, Markov-Chain, game theory, Monte Carlo simulation, Bayesian simulation, and also by a set of predefined stochastic processes (*1*).

Following every failure simulation, whether through partial capacity reduction (*24*)-(*26*) or complete failure (*27*) and (31), the operability of the physical infrastructure measured through a mono-stage mathematical program maximizing network operability index. Consequently, a set of critical links defined and ranked as elements whose failure cause the highest increase in the generalized network cost. The other common

[2] Also known as 'linked-based capacity reduction' or 'link disruption modeling' (*23*).

approach in the element-based vulnerability analysis is partially or completely relaxing a set of links, instead of single link failure, and re-running the model and assessment of the network performance without the set of relaxed links in place. This method is analogous to the single-link failure approach, though its results show a sub-set of network elements having the most impact on infrastructure operability.

1.2.1.2.Grid-based Vulnerability Analysis

Element-based vulnerability analysis has limited performance in metropolitan infrastructures with dense and complex structures. As Jenelius and Mattson argue, in case of extreme events the risk can disrupt 'many or all nearby links,' simultaneously. In (*15*), they advanced a methodology, called 'area-covering disruption analyses,' and covered the study area by 'grid of uniformly shaped and sized cells.' Each cell represents the spatial coverage of an interrupting event and through the simulation, all links within the designated cell are identified and disabled.

1.2.2. Vulnerability Assessment Analysis

A series of research articles considers infrastructure capacity-enhancing strategies that take place prior to extreme events arrival and make the infrastructures more robust to absorb and cope with such events. This category ranges from resource allocation models to reinforcement modeling of network components.

The former investigates the optimal prepositioning of resources which are put in place prior to extreme events. Huang et al. (*9*) solved a maximum service coverage of critical transportation infrastructure. To do so, the complete mixed-integer model is developed through allocation of limited emergency service vehicles. Carmen and Turnquist (*10*)-(*12*), in a series of works, modeled the pre-positioning of emergency resources for use following a disaster. In (*10*), the minimum costs resulting from the selection of the pre-positioning locations and facility sizes, the commodity acquisition, and their shipment's cost is expected. In (*11*), a stochastic mixed integer programming formulation is developed to minimize expected costs of the pre-positioning of emergency supplies for increasing preparedness for natural disasters. In (*12*), an emergency response to disaster threats such as hurricanes is modeled through a two-stage stochastic mixed-integer program and solved by the Lagrangian L-shaped method.

The latter type of pre-event capacity-enhancing strategies concentrates on robustness of urban infrastructures. Murray-Tuite and Mahmassani (*13*) provided a bi-level optimization, non-zero-sum game played by two players to unveil the network's vulnerable elements. In their model, at the bottom-up optimization model (called lower level), a traffic assignment model administered by a transportation management agency seeks minimum system inoperability, whereas an 'evil entity' (top-down model) maximizes network disruptions.

Sullivan et al. (*14*) also advanced a methodological approach that employs different link-based capacity disruption values and identified 'the most critical links' ranking. Jenelius and Mattson (*15*) analyzed the vulnerability of a road network under disruption covering area. They introduced the 'grid-based' approach, as distinct from to single-link failure method, and covered the study area with grids of uniformly shaped and sized cells. Failure then simulated on cells consisting of links and nodes. Yingyan and Zhang (*16*) used tri-level game theory structure among attacker, network user, and defender. To solve the model, they applied an active set algorithm combined with a cutting plan scheme and further explored the network components candidate for robustness strategies.

1.3. Methodology and Model Formulation

The common approach for vulnerability assessment of the critical infrastructures, as briefly discussed, randomly disables the network element(s) or cell, including a number of elements such as links and nodes, and following each component relaxation evaluates the index of network operability. The most vulnerable element is hence, the link in which its failure provides the infrastructure with the highest drop in the functionality metric. This methodology would be valid, if the exogenous shock is only imposed on a limited area and all other network elements (with exception of the relaxed elements) are fully functional. For instance, in cases of single-element failures (e.g. the I-35W Mississippi River bridge collapse in Minnesota, 2007) all the infrastructure's elements were operable except the one under stress. In such one circumstance, other network elements may partially or fully recover the hampered connectedness level, and the network functionality may rebound to the business as usual (BAU) level.

However, this begs the question: what if a large portion of the network faces disruption? In this case, it does not matter what an element's potential vulnerabilities or how efficiently a link contributes to network operability level. Rather, it matters how origin-destination (O-D) pairs are connected and how a set of links provides such connectedness. For example, in case of storm surge and coastal inundation, a large area of a given infrastructure, hence a large number of network elements, become inoperable. Given this situation, detection and capacity-enhancement of the most vulnerable element would not be efficient since the vulnerable element might be surrounded by other inoperable links. So, in such a case, recovering the capacity of the single critical element cannot boost the network functionality metric unless the element is fully connected.

Considering the case study of Manhattan's FSC, we advance a methodology through a mathematical program which computes the most vulnerable element in an infrastructure given i) the typology and topology of random extreme events threatening the case study area and ii) the network's inherent capabilities to withstand and cope with potential shocks. The proposed model is an extension of the well-known fuel replenishment problem (RP). However, the fuel distribution assignment is conditioned on uncertain functionality of the FSC's elements.

Though such functionality is vulnerable to extreme events, it could be protected and possibly enhanced by a robustness-enhancing strategy put in place prior to events' arrival. Through simulation, we relax a predefined number of network elements and through each scenario seek the relaxed-element having the most impact in escalating network performance, if recover or bounce back. In other words, a post-event fuel distribution assignment (second stage variables) is conditioned on pre-event capacity-protecting investment decisions (first stage variables).

The randomness embedded in arrival of events, the separation of pre-event capacity-protecting investment, and post-event fuel replenishment assignment lead the formulation into a bi-stage stochastic programming form. To formulate the general format of the proposed model, we represent the FSC as a direct graph *G (N,*

A): where *N* is a set of nodes with three subsets of supply, demand, and trans-shipment nodes; and *A* is a set of arcs connecting nodes. The general model formulation is shown below.

$$Min \qquad \sum_{s=1}^{S} \mathbb{P}_s[\, E(\sum_{d=1}^{D} U_{d,s})] \tag{1.1}$$

$$s.t. \qquad \sum_{n} \mathrm{I}_n(\alpha) \leq 1 \qquad \forall\, \boldsymbol{\alpha}, s \tag{1.2}$$

The objective function, equation (*1.1*), elaborates the expected unmet demand rate (UDR) in demand node *d* during scenario *s*, indicated as $U_{d,s}$, averaged over all demand nodes and weighted over occurrence probabilities associated with scenarios $\mathbb{P}_s$. Constraint (*1.2*) represents the binary variable indicating the pre-event capacity-restoration investment. This allocates capacity-enhancing strategy α on one of the disrupted elements *n*. The proposed model seeks an optimum interaction between pre-event investments and post-event fuel distribution patterns. The pre-event investment ($\boldsymbol{\alpha}$) and post-event fuel routing task (X_s) are being determined, simultaneously, when the model seeks a set of pre-positioning of assets that optimizes fuel distribution assignment.

1.4. Illustrative Case Study

The motor fuel distribution network in Manhattan includes 29 gas stations which all are branded and supplied by major companies' terminals/refineries. Supply nodes, eighteen in total, are entirely located out of Manhattan, either in adjacent boroughs or in the State of New Jersey. Terminals and fueling stations are connected through the transportation network containing inner-city passages and interstate highways. Figure 1 represents the FSC of Manhattan, layered in 2,475 square miles, including 685 trans-shipment nodes and 2,103 connecting arcs.

Modeling hurricanes aftermaths on Manhattan FSC requires us to study the threats in three pillars: i) type and frequency, ii) corresponding vulnerable locations, and iii) expected intensity. Adapted from 'NYS Standard Multi-Hazard Mitigation Plan' and the 'Sea, Lake and Overland Surges from Hurricanes'

(SLOSH) model of NYC, Figure 2 shows hurricane categories, corresponding storm surge inundation zones (each category's vulnerable zones), and expected intensity of potential hurricanes in both metrics of wind intensity and surge height. As shown in Figure 2, Manhattan FSC is vulnerable to 4 categories of hurricanes ranging from category 1 with the lowest impact magnitude to category 4 with the highest. To determine the return period of hurricanes categories, we used 'The Hazards U.S. Multi-Hazard' (Hazus-MH), a nationally applicable standardized methodology containing models for estimating potential losses from hurricanes. Extracting from Hazus-MH, the arrival chance for each hurricane category in NYC could be summarized as the following.

Table 1. Scenario Description and Occurrence Chances

Event	Description	Arrival chance
1	BAU (no extreme event)	0.9474
2	Hurricane Category 1	0.0245
3	Hurricane Category 2	0.0145
4	Hurricane Category 3	0.01
5	Hurricane Category 4	0.0036

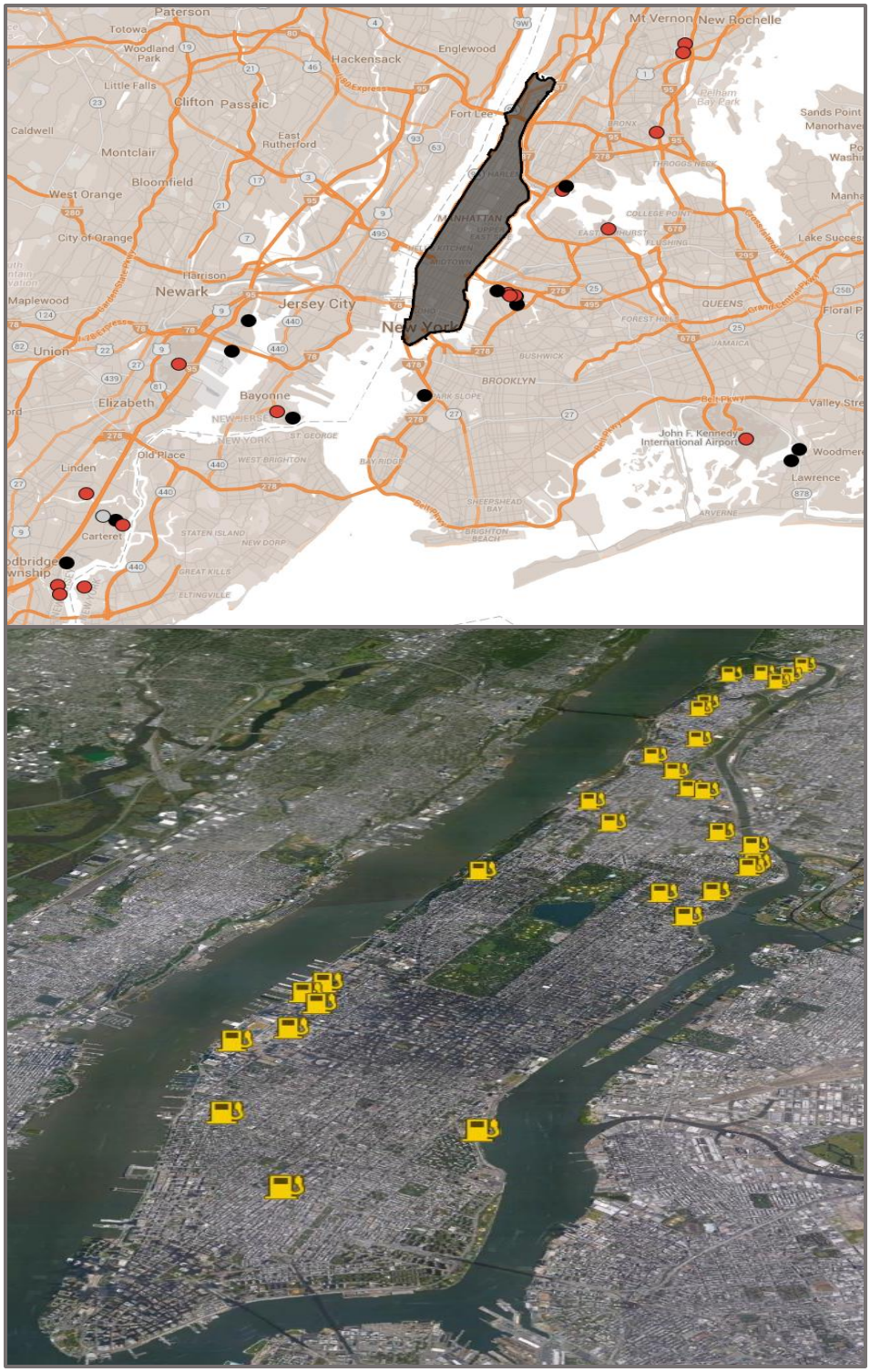

Figure 1. Manhattan FSC. Top: Supply nodes including terminals and refineries. Bottom: Demand nodes including gas stations.

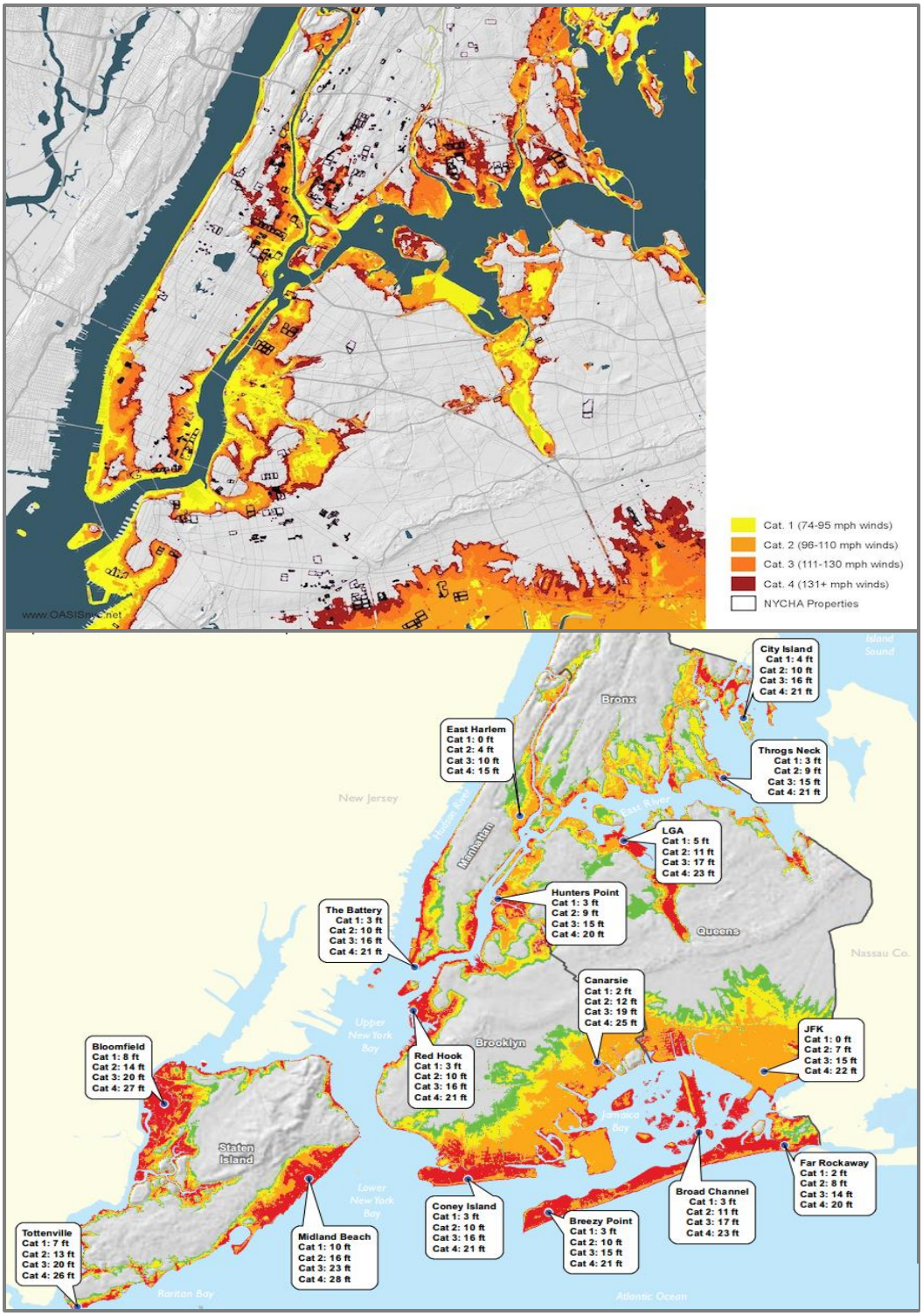

Figure 2. Hurricane maps. Top: Hurricanes corresponding vulnerable zones. Bottom: Expected intensity by hurricane categories.

Through the various hurricane categories, the FSC's elements perform differently. Precisely, a given network element might be interrupted by a particular category of hurricane if the element is i) located in the hurricane's corresponding flooding zone and ii) vulnerable to the level of impact imposed by such a category. The first condition—the geographic location of elements—is investigated by projecting the SLOSH hurricane vulnerability zones as GIS layers onto the FSC map.

Investigation of the second condition—vulnerability of elements in face of hurricanes—however, requires detailed information about the robustness level of each element in the face of hurricane categories. Due to lack of the information in regards to elements' robustness conditions, we assume the FSC's elements are fully vulnerable against hurricanes' aftermath, meaning that a given element fails if a hurricane occurs, no matter what the category of hurricane. This assumption could be relaxed, through a line of simulations (e.g. Markov Chain) which assume elements may receive partial disruptions due to arrival of hazards.

Table 2. Nomenclature

Sets	
$\{n\} = \{1, 2, ..., N\}$	Scenarios
$\{\alpha\} = \{1, 2, ..., A\}$	Capacity-enhancing (investment) strategies
$\{s\} = \{1, 2, ..., S\}$	Supply nodes (terminals)
$\{t\} = \{1,2, ..., T\}$	Trans-shipment nodes
$\{d\} = \{1,2, ..., D\}$	Demand nodes (gas stations)
$\{k\} = \{1,2, ..., K\}$	Fuel types
Parameters	
$\mathbb{P}_n$	Chance of occurrence of scenario n
$\mathbb{L}$	A large number
$F_{d,n}^{k}$	Demand of commodity k in demand node d during scenario n
$F_{s,n}^{k}$	Supply of commodity k in supply node s during scenario n
$NO(d^k)$	Number of demand nodes (gas stations) in the city of Manhattan

$C^{k}_{s,t,n}$	Distance between supply node *s* and trans-shipment node *t* during scenario *n*
$C^{k}_{t,tt,n}$	Distance between trans-shipment nodes during scenario *n*
$C^{k}_{t,d,n}$	Distance between trans-shipment node *t* and demand node *d* during scenario *n*
$O^{k}_{s,n}$	Operability of node *s* during scenario *n*. 1 if operable, 0 otherwise
$O^{k}_{d,n}$	Operability of node *d* during scenario *n*. 1 if operable, 0 otherwise
$O_{s,t,n}$	Operability of arc (*s*,*t*) during scenario *n*. 1 if operable, 0 otherwise
$O_{t,tt,n}$	Operability of trans-shipment arc during scenario *n*. 1 if operable, 0 otherwise
$O_{t,d,n}$	Operability of arc (*t*,*d*) during scenario *n*. 1 if operable, 0 otherwise
$W_{s,t,n}$	Nominal capacity of arc (*s*,*t*) during scenario *n*
$W_{t,tt,n}$	Nominal capacity of the transshipment arc during scenario *n*
$W_{t,d,n}$	Nominal capacity of arc (*t*,*d*) during scenario *n*
	Decision variables
$U^{k}_{d,n}$	UDR (unfill rate) corresponding to fuel type *k* in demand node *d* during scenario *n*
$X^{k}_{s,t,n}$	Flow type *k* on arc (*s*,*t*), during scenario *n*
$X^{k}_{t,tt,n}$	Flow type *k* on transshipment arc, during scenario *n*
$X^{k}_{t,d,n}$	Flow type *k* on arc (*s*,*d*), during scenario *n*
$\mathbb{V}$	Number of investment strategies
$I^{k,\alpha}_{s}$	Binary variable; 1 if investment strategy α is chosen for facilities corresponding to fuel type *k* at supply node *s*, 0 otherwise
$I^{k,\alpha}_{d}$	Binary variable; 1 if investment strategy α is chosen for facilities corresponding to fuel type *k* at demand node *d*, 0 otherwise
$I^{\alpha}_{s,t}$	Binary variable; 1 if investment strategy α is chosen for arc (*s*,*t*), 0 otherwise
$I^{\alpha}_{t,tt}$	Binary variable; 1 if investment strategy α is chosen for transshipment arc, 0 otherwise
$I^{\alpha}_{t,d}$	Binary variable; 1 if investment strategy α is chosen for arc (*t*,*d*), 0 otherwise

Employing the notation synopsized in Table 2, Manhattan's FSC vulnerability analysis is formulated as the following bi-stage stochastic program.

Min $\sum_{n=1}^{N} \mathbb{P}_n [\mathbb{L} \frac{\sum_{d=1}^{D}\sum_{k=1}^{K} U_{d,n}^{k}}{\sum_{k=1}^{K} NO(d^k)} + \sum_{s=1}^{S}\sum_{t=1}^{T}\sum_{k=1}^{K} X_{s,t,n}^{k} C_{s,t,n}^{k} + \sum_{t=1}^{T}\sum_{tt=1}^{TT}\sum_{k=1}^{K} X_{t,tt,n}^{k} C_{t,tt,n}^{k} + \sum_{t=1}^{T}\sum_{d=1}^{D}\sum_{k=1}^{K} X_{t,d,n}^{k} C_{t,d,n}^{k}]$ (*1.3*)

s.t. $\mathbb{V} = \sum_{s=1}^{S}\sum_{k=1}^{K} I_s^{k,\alpha} + \sum_{d=1}^{D}\sum_{k=1}^{K} I_d^{k,\alpha} + \sum_{s=1}^{S}\sum_{t=1}^{T} I_{s,t}^{\alpha} + \sum_{t=1}^{T}\sum_{tt=1}^{TT} I_{t,tt}^{\alpha} + \sum_{t=1}^{T}\sum_{d=1}^{D} I_{t,d}^{\alpha}$ (*1.4*)

$\mathbb{V} \leq 1$ (*1.5*)

$U_{d,n}^{k} = (F_{d,n}^{k} - \sum_{t=1}^{T} X_{t,d,n}^{k}) / F_{d,n}^{k}$ (*1.6*)

$F_{s,n}^{k}[O_{s,n}^{k} + (1-O_{s,n}^{k})\, I_s^{k,\alpha}] \geq \sum_{t=1}^{T} X_{s,t,n}^{k}$ $\forall\, s, n, k$ (*1.7*)

$F_{d,n}^{k}[O_{d,n}^{k} + (1-O_{d,n}^{k})\, I_s^{k,a}] \geq \sum_{t=1}^{T} X_{t,d,n}^{k}$ $\forall\, d, n, k$ (*1.8*)

$\sum_{k=1}^{K} X_{s,t,n}^{k} \leq W_{s,t,n}[O_{s,t,n} + (1-O_{s,t,n})\, I_{s,t}^{\alpha}]$ $\forall\, s, t, n$ (*1.9*)

$\sum_{k=1}^{K} X_{t,tt,n}^{k} \leq W_{t,tt,n}[O_{t,tt,n} + (1-O_{t,tt,n})\, I_{t,tt}^{\alpha}]$ $\forall\, t, tt, n$ (*1.10*)

$\sum_{k=1}^{K} X_{t,d,n}^{k} \leq W_{t,d,n}[O_{t,d,n} + (1-O_{t,d,n})\, I_{t,d}^{\alpha}]$ $\forall\, s, t, n$ (*1.11*)

$X_{s,t,n}^{k} \geq 0$ $\forall\, k, s, t, n$ (*1.12*)

$X_{t,tt,n}^{k} \geq 0$ $\forall\, k, t, tt, n$ (*1.13*)

$X_{t,d,n}^{k} \geq 0$ $\forall\, k, t, d, n$ (*1.14*)

As discussed, the primary goal of this model is to minimize the system inoperability (UDR) in times of disaster, while the secondary goal is to minimize the fuel distribution cost. Consequently, the objective (*1.3*) minimizes the expected UDR, 'unfill rate', as well as fuel distribution costs. Both values are weighted over the occurrence probabilities of events.

Within the objective function, one factor is embedded: scalar $\mathbb{L}$, as a large number, prioritizes the least expected unfill rate on fuel distribution costs. Constraint (*1.4*) captures the number of capacity restoration

strategies chosen by model. Constraint (*1.5*) simply limits the number of strategies to one. Constraint (*1.6*) elaborates on an inoperability index (UDR) which is equal to the ratio of unsatisfied demand to expected demand averaged over all gas stations. Constraints (*1.7*) -(*1.8*) indicate flow conservations in terminals and gas stations. Constraint (*1.7*) shows the upper-bound of terminals' outgoing flows on terminals' available supply. This constraint also conditions the operability of a given terminal, *s*, on the following condition: terminal *s* must be robust, hence operable, against the scenario *n*; if not, a capacity restoration strategy must be implemented to maintain the functionality of this terminal. Constraint (*1.8*) embodies the same concept for gas stations. Constraints (*1.9*) -(*1.11*) govern the flow capacity of arcs and restrict distributed flows so they do not exceed the arcs' nominal capacities. Similar to the concept used in flow conservation constraints, a given arc's functionality in scenario *n* is conditioned on either robustness of that arc against scenario *n* or implication of the capacity restoration strategies. Ultimately, constraints (*1.12*) -(*1.14*) reassure the non-negativity of flows.

1.5. Computational Experiments

The FSC of Manhattan, similar to other NYC infrastructures, is extremely vulnerable to exogenous shocks such as extreme weather episodes. To investigate the vulnerability of this infrastructure and explore the optimum investment setting towards robust functioning in time of disaster, the proposed model is applied to the case study discussed in the section 4. The results driven by the proposed method are compared to the output of the classic vulnerability analysis technique, conclusion are drawn, and suggestions made to improve further research in this arena. Two models are set to experiment and analyze the vulnerability of the Manhattan's FSC. Model *I* represents results driven by the common approach to this class of problem. Through this model, three experiments are performed and compared, as shown in Figure 3, Left. The first experiment shows how strengthening up to ten vulnerable elements in the transportation network increases the FSC operability index.

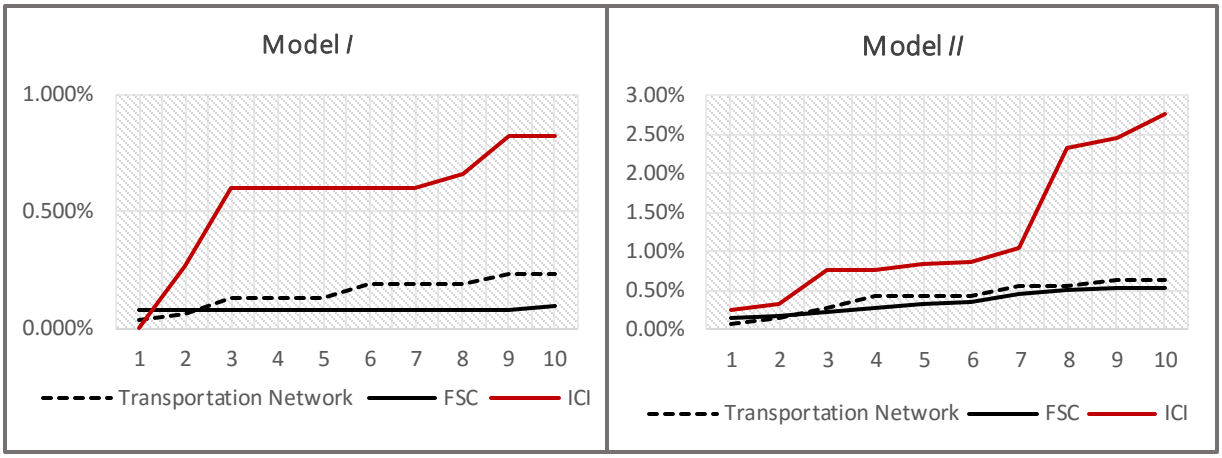

Figure 3. Left: Experiments results of traditional technique; Right: Experiments results of traditional technique

The enhancement of the most vulnerable elements in the transportation network (arcs) improves the network performance by less than 0.6 percent. Whereas, as resulted by the second experiment, enhancing up to ten vulnerable elements in supply chain infrastructures (i.e. terminals, refineries, distribution facilities, and service stations) recovers 0.7 percent of the hampered operability. Considering both networks as an interdependent critical infrastructures (ICI), experiment 3 shows 0.8 percent raise on the network performance index. The ICI's operability demonstrates inevitable higher improvement when resources are allocated through both networks of transportation and supply-chain.

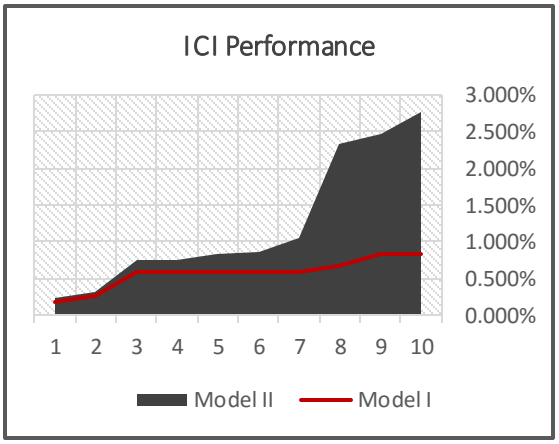

Figure 4. Comparison of the results driven by model I and model II

This clearly emphasizes the importance of the modeling within the context of multi-layer infrastructures. In the last experiment of the model *I*, the existing physical interdependency across the infrastructures leads the optimization model to allocate resources across both of the systems. The same set of experiments is performed under the proposed method. As discussed, we proposed two modifications for the common modeling technique: i) considering the connectedness of the O-D pairs and ii) allocating the available resources across the network elements with respect to the vulnerability of elements in different stochastic scenarios. The experiments' outputs of the model *II* are shown in Figure 3, right. The resource allocation trends across the experiments are similar to the patterns in the first model; the first two experiments provide the ICI with the lower level of operability enhancement with comparison to the last experiment. However, the contribution of the investment strategies on the infrastructure's overall functionality is negligible.

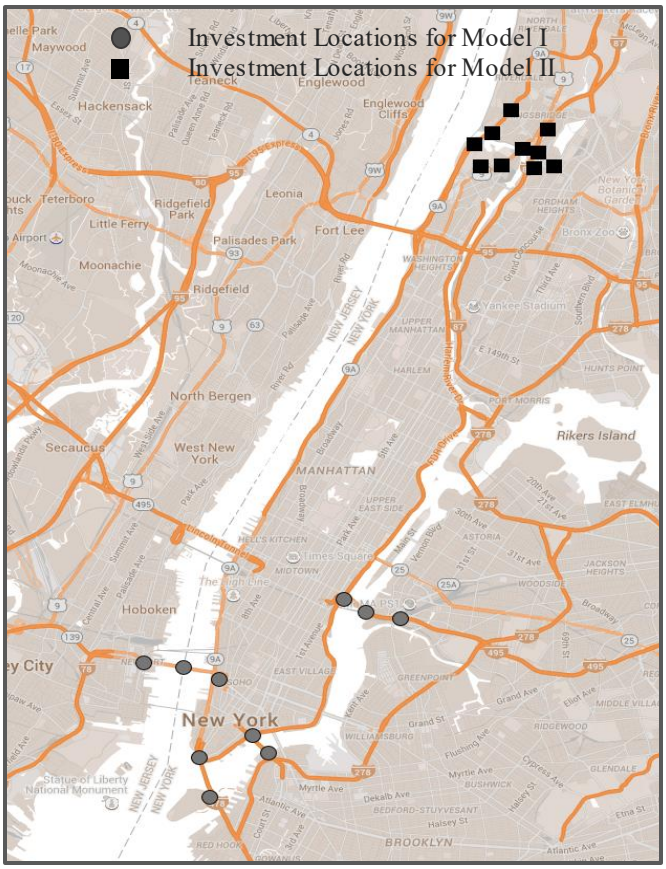

Figure 5. Resource allocation through both models

Drawing a comparison between the proposed method and the common technique in vulnerability analysis, through the second model the network recovers up to 2.76 percent of the hampered functionality, while the first model restores less than one-third of this rate. Though the results of the second model are clearly improved comparing to the common technique's output, in particular for the ICI's capacity-enhancing strategies, capacity-enhancing rates vary based on how the network is graphed and how the robustness strategies are set by the modeler.

Aside from the different impacts that models have on network performance, the arrangement and location of the proposed enhancing-strategies are also different. The first model concentrates the investing resources mainly on critical bridges connecting the Borough of Manhattan to Brooklyn and Jersey City. The reason for such resource allocation density is the criticality and the connectedness ability of the South Manhattan bridges in linking the Borough's service stations to the out-of-the Borough supplying nodes.

In the case of BAU or in the time of man-made hazards, such as terrorist attacks all other network elements are operable, therefore, the functionality of these bridges is the most vital factor for the commodity distribution. However, in the face of extreme weather episodes or large scale flooding, maintaining the operability of these bridges cannot bounce back the system performance since the adjacent arcs to these bridges are all relaxed and out of service. Hence, finding the most critical element cannot be an optimum strategy as long as the given element is the only disturbed link between a connecting O-D pair.

As shown in the Figure 5, the second model distributes resources on the north side of the Borough since the density of vulnerable land parcels in the North Manhattan is relatively low. Through the proposed method—model *II*—flow supplied by terminals located on The Bronx and distributed through the Manhattan via arcs are maintained. Whereas, the first model—model *I*—supplies the flow from the New Jersey terminals and transships through the most vulnerable land parcels in the South Manhattan.

1.6. Conclusion

To expand our understanding of the concept of vulnerability analysis and to explore its application in metropolitan critical infrastructures, this paper models Manhattan's motor fuel supply-chain and advances

a methodology towards identifying the network's most vulnerable element(s). The proposed method is performed in two steps. The former step is mainly focused on understanding the case study and data collection by i) drawing the motor fuel supply-chain network serving the City of Manhattan through a Visual Basic-coded application programming interface (VB-API) and ii) studying the extreme weather episodes potentially threatening the case study area and investigating their corresponding aftermaths on FSC's elements. Furthermore, the latter step performs a mathematical program to seek the optimum set of capacity-enhancing strategies to reduce and otherwise manage infrastructures' vulnerabilities.

Mathematically, the proposed optimization model is developed through a bi-stage, mixed-integer, stochastic form. The variables are split into two stages: asset allocation tasks which are the first stage variables and fuel distribution assignment as the second stage variables. The second stage variables are conditioned on the first stage decisions, where resources are allocated to produce the optimum set of second stage decisions. A series of computational experiments has also been performed to investigate the network functionality given various scenarios. The results illustrate how the proposed method enhances the capability of the network to better withstand hazards, compared with the common approach in vulnerability analysis studies.

REFERENCES

1. Turnquist, Mark, and Eric Vugrin. "Design for resilience in infrastructure distribution networks." Environment Systems & Decisions 33, no. 1 (2013): 104-120.
2. Lee, Hau L. "The triple-A supply-chain." Harvard business review 82, no. 10 (2004): 102-113.
3. Bruneau, Michel, et al. "A framework to quantitatively assess and enhance the seismic resilience of communities." Earthquake spectra 19.4 (2003): 733-752.
4. Ponomarov, Serhiy Y., and Mary C. Holcomb. "Understanding the concept of supply-chain resilience." The International Journal of Logistics Management 20, no. 1 (2009): 124-143.
5. Soni, Umang, and Vipul Jain. "Minimizing the vulnerabilities of supply-chain: A new framework for enhancing the resilience." In Industrial Engineering and Engineering Management (IEEM), 2011 IEEE International Conference on, pp. 933-939. IEEE, 2011.
6. Tomlin, Brian. "On the value of mitigation and contingency strategies for managing supply-chain disruption risks." Management Science 52.5 (2006): 639-657.
7. Jessup, Eric, et al. Development and analysis of a GIS-based statewide freight data flow network. No. WA-RD 730.1. Washington State Department of Transportation, 2009.
8. Tang, Christopher S. "Robust strategies for mitigating supply-chain disruptions." International Journal of Logistics: Research and Applications 9, no. 1 (2006): 33-45.
9. Huang YX, Fan Y, Cheu RL. Optimal allocation of multiple emergency service resources for critical transportation infrastructure protection. Transportation Research Record 2007; 2022: 1–8.
10. Rawls, Carmen, Mark Alan Turnquist. 2012. "Pre-positioning and Dynamic Delivery Planning for Short-term Response following a Natural Disaster." Socio-Economic Planning Sciences 46 (1): 46-54.
11. Rawls, Carmen G., Mark Alan Turnquist. 2011. "Pre-positioning Planning for Emergency Response with Service Quality Constraints." OR Spectrum 33 (3): 481-498.

12. Rawls, Carmen G., Mark Alan Turnquist. 2010. "Pre-positioning of Emergency Supplies for Disaster Response." Transportation Research, Part B 44: 521-534.

13. Murray-Tuite, Pamela M., and Hani S. Mahmassani. "Methodology for determining vulnerable links in a transportation network." Transportation Research Record: Journal of the Transportation Research Board 1882.1 (2004): 88-96.

14. Sullivan, J. L., et al. "Identifying critical road segments and measuring system-wide robustness in transportation networks with isolating links: A link-based capacity-reduction approach." Transportation Research Part A: Policy and Practice 44.5 (2010): 323-336.

15. Jenelius, Erik, and Lars-Göran Mattsson. "Road network vulnerability analysis of area-covering disruptions: A grid-based approach with case study." Transportation research part A: policy and practice 46.5 (2012): 746-760.

16. Lou, Yingyan, and Lihui Zhang. "Defending transportation networks against random and targeted attacks." Transportation Research Record: Journal of the Transportation Research Board 2234.1 (2011): 31-40.

17. Chen, Lichun, and Elise Miller-Hooks. "Resilience: an indicator of recovery capability in intermodal freight transport." Transportation Science 46.1 (2012): 109-123.

18. Vugrin, Eric D., Mark A. Turnquist, and Nathanael JK Brown. Optimal recovery sequencing for enhanced resilience and service restoration in transportation network. No. SAND2013-4852J. Sandia National Laboratories (SNL-NM), Albuquerque, NM (United States), 2013.

19. Miller-Hooks, Elise, Xiaodong Zhang, and Reza Faturechi. "Measuring and maximizing resilience of freight transportation networks." Computers & Operations Research 39, no. 7 (2012): 1633-1643.

20. A common approach for the shock simulation techniques in scenario-specific studies is based on the link failures, whether through single link failure or multiple-link failures.

21. Simonsen, Ingve, et al. "Transient dynamics increasing network vulnerability to cascading failures." Physical review letters 100.21 (2008): 218701.

22. Chen, Anthony, et al. "Network-based accessibility measures for vulnerability analysis of degradable transportation networks." Networks and Spatial Economics 7.3 (2007): 241-256.

23. Sullivan, J. L., et al. "Identifying critical road segments and measuring system-wide robustness in transportation networks with isolating links: A link-based capacity-reduction approach." Transportation Research Part A: Policy and Practice 44.5 (2010): 323-336.

24. Asakura, Y. "Reliability measures of an origin and destination pair in a deteriorated road network with variable flows." Transportation Networks: Recent Methodological Advances. Selected Proceedings of the 4th EURO Transportation Meeting. 1999.

25. Chen, Anthony, et al. "Capacity reliability of a road network: an assessment methodology and numerical results." Transportation Research Part B: Methodological 36.3 (2002): 225-252.

26. Poorzahedy, Hossain, and Sayed Nader Shetab Bushehri. "Network performance improvement under stochastic events with long-term effects." Transportation 32.1 (2005): 65-85.

27. Beheshtian, A., and Donaghy, K. (2016). Planning Resilient Motor Fuel Supply-Chain. Transportation Research Record. In Press, under second review.

28. Snyder, Lawrence V., and Mark S. Daskin. "Models for reliable supply chain network design." Critical Infrastructure. Springer Berlin Heidelberg, 2007. 257-289.

29. Scott, Darren M., et al. "Network robustness index: a new method for identifying critical links and evaluating the performance of transportation networks." Journal of Transport Geography 14.3 (2006): 215-227.

30. Taylor, Michael AP, and Glen M. D'Este. Transport network vulnerability: a method for diagnosis of critical locations in transport infrastructure systems. Springer Berlin Heidelberg, 2007.

31. Matisziw, Timothy C., Alan T. Murray, and Tony H. Grubesic. "Evaluating vulnerability and risk in interstate highway operation." Transportation research board 86th annual meeting. No. 07-0340. 2007.

32. Holmgren, Åke J. "A framework for vulnerability assessment of electric power systems." Critical Infrastructure. Springer Berlin Heidelberg, 2007. 31-55.

33. Grubesic, Tony H., Alan T. Murray, and Jessica N. Mefford. "Continuity in critical network infrastructures: accounting for nodal disruptions." Critical Infrastructure. Springer Berlin Heidelberg, 2007. 197-220.

34. O'Kelly, Morton E., and Hyun Kim. "Survivability of commercial backbones with peering: a case study of Korean networks." Critical Infrastructure. Springer Berlin Heidelberg, 2007. 107-128.

35. Lam, W., Ning Zhang, and Hong K. Lo. "A reliability-based user equilibrium model for traffic assignment." Critical Infrastructure (2007): 151-171.

36. Rezaei Moghaddam, M. H., et al. "Mapping susceptibility landslide by using the weight-of-evidence model: a case study in Merek Valley, Iran." Journal of Applied Sciences 7 (2007): 3342-3355.

37. Matisziw, Timothy C., and Alan T. Murray. "Modeling s–t path availability to support disaster vulnerability assessment of network infrastructure." Computers & Operations Research 36.1 (2009): 16-26.

CHAPTER 2

PLANNING A RESILIENT MOTOR FUEL SUPPLY CHAIN

2.1. Introduction

Among metropolitan infrastructures, the transportation network is critical, affecting a metropolitan area's performance and playing a crucial role in regional and national wellbeing. Transportation infrastructures, yet do not perform exclusively and their output relies on functionality of the interconnected networks such as motor fuel supply-chain (FSC). Despite the vitality of functional interdependent critical infrastructures, keeping these networks operable is a complex task. This complexity however is multifold and is driven by a number of causes.

First, urban infrastructures are complex by nature. The large size of infrastructures in addition to dynamic behavior and existing interdependencies across interlinked infrastructures make metropolitan infrastructures complex to design and operate. Second, a majority of urban America's infrastructures are nearing the ends of their service lives. Aging and in many cases over-capacitated infrastructures introduce a new class of operational difficulty, when the nominal service rates is either unachievable or not adequate to meet the actual demand.

Third, urban infrastructures are vulnerable to sudden extreme events. Indirect failures rippled from interdependent infrastructures and direct inoperabilities imposed by extreme exogenous shocks (e.g., terrorist attacks or severe weather episodes) are examples causing different levels of disruption or even failures across the networks' elements. Any one of these complexity sources arguably introduces a new line of challenges to infrastructures' designer and operators who are willing to i) optimize the functionality of a given infrastructure in the state of 'business as usual' (BAU) and ii) protect and possibly maintain the infrastructures' operability under an extreme event's attack.

For example, inevitable vulnerability of the New York City (NYC) to Atlantic hurricanes and tropical storms has faced the City's infrastructures to frequent failures and caused considerable economic loss at

regional and national levels. In case of hurricane Sandy, the storm battered the NYC's critical infrastructures with heavy rain, strong winds, and record storm surges. In consequence, a number of the City's physical networks faced major interruptions, in particular, the City's FSC faced extensive and broad disruptions; refineries and terminals lost power and were damaged, and pipelines and power grid were shut down, all of which led to widespread gas station closures. Despite the early speculations that these closures were due primarily to power outages that prevented stations from pumping gas, the larger problem turned out to be that stations simply had no gas to pump. According to the U.S. Energy Information Administration (EIA 2012), from the days of the 4th through 11th following the Sandy, 67-28% of gas stations across the New York metropolitan area and with a larger ratio in the Borough of Manhattan did not have gasoline available for sale.

The reason behind the post-Sandy supply deficit was the inoperability of the fueling infrastructure's key-elements; in addition to a total of twenty-eight terminals that were affected by Sandy, thousands of roads were closed because of downed power lines or tree limbs hampering the ability of trucks to get to open terminals or deliver fuel, even if they were able to obtain it (NACS 2013[3]). The station closures, and the long lines at the stations that did have gas, not only limited mobility and slowed economic activity, they also hampered recovery efforts and caused cascading failures across other critical infrastructures like transportation and transit.

In response to the past decade's super-storms that struck NYC, notably following hurricane Sandy, the State government announced the appointment of three commissions[4] to 'improve the State's emergency preparedness and response capabilities and strengthen the State's infrastructure to withstand natural disasters[5].' The commissions' reports were released within a year after super-storm Sandy and recognized

[3] National Association of Convenience Stores (2013) http://www.nacsonline.com/YourBusiness/FuelsReports/GasPrices_2013/Pages/How-Hurricane-Sandy-Affected-the-Fuels-Industry.aspx.

[4] NYS 2100 Commission, NYS Respond Commission, and NYS Ready Commission

[5] www.governor.ny.gov/news/governor-cuomo-announces-commissions-improve-new-york-states-emergency-preparedness-and

the NYC's motor fueling infrastructure as a vulnerable-critical network in need of a resilient platform to better withstand the upcoming extreme weather episodes. Following such recognition, a large number of risk assessment and disaster preparedness studies have been performed to analyze the functionality of NYC's critical infrastructures when stressed or under attack. In spite of this trend, the sheer complexity of critical infrastructures combine with inevitable ambiguity corresponds to extreme events arrival left many uncertainties in regards to modeling this problem domain.

In this paper, we take on this challenge and exercise the concept of network resilience within the context of motor fuel supply-chain management. Following efforts made by Turnquist et al. (2013), we develop a mathematical program to analyze practical strategies and optimally allocate resources to maximize Manhattan FSC's resilience in time of hurricanes. These strategies are developed within three pillars of absorption, adaptation, and restoration. As a set of complementary strategies, resilience-enhancing strategies (RES) take place pre-, during-, and post-event(s) to optimally manage inoperability imposed by potential severe weather episodes. The uncertainty in arrival of extreme events combine with the separation of pre-event investments and post-event network's performance lead the proposed optimization model to a stochastic bi-stage form where fuel replenishment/distribution task (second stage variables) is conditioned on investment decisions that are made within the first stage. The key-objective of the proposed model is to investigate an optimum investing strategy which provides the FSC with maximum resilience in the face of extreme weather episodes.

2.2. Literature review

Holling (1973), a theoretical ecologist, defines the term resilience as a 'measure of the persistence of systems.' Since then, this term has been conceptualized in a number of disciplines ranging from economics and politics to engineering and planning. Within the pool of supply-chain and risk management studies, however, resilience is defined as a system property which encapsulates several characteristics. Lee (2004) presented a 'triple-A' aspects of resilient supply-chain as agility, adaptability, and alignment. Bruneau et al. (2003) elaborated four 'complementary measures' of robustness, redundancy, resourcefulness, and

rapidity in recovery. Ponomarov and Holcomb (2009) also discussed over three steps of readiness, response, and recovery, and Soni and Jain (2011) introduced flexibility, visibility, collaboration, adaptability, and sustainability as required attributes to support the supply-chain resilience. Lastly, Turnquist and Vugrin (2013) explored the concept of resilience in supply-chain domain and explored 'resilience-enhancing investments' through three lines of absorption, adaptation, and restoration activities.

Despite the 'divergent definitions' and 'conceptual vagueness' of the term resilience (Tomlin 2006; Jessup et al. 2009; Tang 2006), there are a few common grounds within a majority of the research areas: i) resilience, as an aspect of the systems, represents the capability of infrastructures to experience minimum inoperability in time of disaster and bounce back optimally into the pre-disturbance state, and ii) RES are conceptualized within three time windows of pre-, during- and post-shock. By relying on the existing literature, we recognize the term resilience as a system's property to better withstand and absorb, efficiently adapt to, and quickly/cheaply recover from the inoperability imposed by extreme events. Besides the illustrative and conceptual studies, a number of quantitative methods have been developed to address the critical infrastructures' resilience. Herein, we summarize these quantitative approaches into three threads:

2.2.1. Resilience-enhancing strategies a priori of an event arrival

A series of research studies the RES that take place prior to extreme events' arrival. This category consists of vulnerability studies and resource allocation models. The former type, networks vulnerability, studies the systems' resilient capacity by identifying the most vulnerable element(s) given arrival of a disrupting event. The general approach of this method is based on simulating, whether exogenous or endogenous, shocks, relaxing the functionality of the network element(s), and identifying those elements which impose the most inoperability on the system's well-being.

Sullivan et al. (2010) investigated the most critical links in a regional transportation network with 335 traffic analysis zones (TAZ) and approximately 1792 links. They investigated 'an ideal capacity-disruption range' that can be used to compare networks of different sizes and topologies and showed that 'the rank-ordering of the most critical links' varied through different capacity-disruption ranges. Jenelius and Mattson (2012)

analyzed the vulnerability of the Swedish road network under disruption covering area. They introduced a 'grid-based' approach, as opposed to the 'link-failure' method, and covered the study area with grids of uniformly shaped and sized cells. Then, they simulated failures on cells consisting links and nodes, instead of just links.

Murray-Tuite and Mahmassani (2004) advanced a methodology for determining the vulnerable elements in a transportation network of 8 links. Through a bi-level mathematical program, they modeled a non-zero-sum game played by two players. At the bottom-up model, the transportation management agency seeks the system's optimal traffic assignment. Whereas an 'evil entity', in the top-down model, maximizes the network disruptions by targeting a set of links. Lou and Zhang (2011) used tri-level game theory structure among attackers, network users, and defenders to model the random and targeted attacks on the Sioux Falls transportation network. They studied the reliability of travel time and unsatisfied travel demand through a tri-level game played by the travelers, attacker, and planner.

The second class of modeling, resource allocation models, investigate the allocation of resources/assets which provides the disrupted infrastructure with an optimum functionality. This happens through pre-positioning of resources directly on those elements which have the most impact on the system's functionality if stressed or under attack. Contrary to vulnerability studies which consider a single disruption scenario, this class of modeling may seek an allocation of resources optimum against several disruption scenarios by considering all the possible events simultaneously. In case of the multi-scenario models, the solutions aren't necessarily optimal against a particular event which is the case in the networks vulnerability studies. Rawls and Turnquist (2010, 2011, 2012), in a series of studies, modeled the pre-positioning of emergency resources. In their earliest study, Rawls and Turnquist (2010) modeled an emergency response to disaster threats (hurricanes) in a network of 30 nodes and 58 links in the southeastern US. They used a bi-stage stochastic mixed-integer program, where in the first stage, they examined the storage facility locations and sizes, as well as stocking decisions for various types of supplies. While for the second stage, they analyzed the distribution of available supplies in response to random events and network conditions.

In their following study, Rawls and Turnquist (2011) developed a stochastic mixed integer programming to minimize the expected costs of the pre-positioning of emergency supplies in the same network they studied in 2010. In their last study, Rawls and Turnquist (2012), they optimized the distribution pattern of the emergency supplies and extended their previous static models to dynamic approach where the arrival of evacuees at shelter locations vary over time. To do so, they expected the minimum costs resulting from the selection of the pre-positioning locations and facility sizes, the commodity acquisition, and their shipment.

2.2.2. Post-event strategies

A line of studies assesses the post-event resilience-enhancing actions under the umbrella of recovery/restorative planning. Chen and Miller-Hooks (2012) studied the intermodal freight network's ability to recover from disruptions. To do so, they proposed a mixed-integer stochastic model to identify the 'optimum post-event course of actions'. Vugrin et al. (2014) studied the optimum recovery sequencing through introducing a bi-level optimization model. They extended the scheduling problem, where they assigned a value on 'partial operation' of a distribution network consisting of 8 links. Through the proposed bi-level model, the bottom-up model solves a typical network min-cost problem and the top-down model searches for an optimum sequence of restoration scenarios.

2.2.3. Strategies pre-, during-, and post-event

While the first two categories of studies, separately, consider pre- and post-event actions, the third thread of methods explores a range of pre- and post-event actions, as well as a series of strategies taken place during an event, simultaneously. Miller-Hooks et al. (2012) extended their previous work (Chen and Miller-Hooks, 2012) and in addition to the post-event actions, they considered what potential actions might be taking place prior to events. They modeled the intermodal freight network through a 'virtual highway network' of 11 arcs and 17 O-D pairs. They solved a two-stage non-linear stochastic integer program which maximizes the flowed double-stack containers given i) the optimal investment decision that are planned in a priori to a disaster and ii) the optimal recovery actions taken place post-disaster.

Turnquist and Vugrin (2012) focused on the dynamic state of the network and introduced a bi-stage stochastic optimization model for the resilient network infrastructure. For a supply-chain network of 39 customers and 4 distribution centers, they drew a distinction between decisions that take place pre- and post-event. To identify the pre-event actions, they studied a set of investment strategies to enhance absorptive, adaptive, and restorative capacities and solved a mathematical program for the optimum post-event transshipment decisions of commodities from suppliers to markets. They conditioned the second stage variables (recovery actions) on pre-event investments and examined the optimum first stage variables which provide 'the most efficient potential random outcomes'. While the concept of resilience has been applied in a range of supply-chain contexts and developed through a number of methodologies, herein, we advance an analytical planning tool to neutralize or otherwise control the negative consequences Manhattan's motor fuel supply chain expects following extreme weather episodes. In this work, we assume an actual-size network and have collected first-hand information of supply rate at terminals/refineries and demand rate at fueling stations. Further, we employ the floodplain maps produced by computerized numerical tools to model the hurricanes-induced vulnerabilities on the case study's elements.

Further, the proposed model, as of our knowledge, is the only developed analytical interface between resilience-enhancing policies and the infrastructures' mechanism to i) simulate the impact of currently-employed and funded resilience-enhancing strategies on Manhattan's overall wellbeing in time of hurricane and ii) investigate an optimum set of strategies yielding the maximum resilience to Manhattan's FSC.

2.3. Illustrative case study

2.3.1. Drawing the FSC network

Manhattan currently has twenty-nine gas stations, all branded and supplied by the major oil companies. These stations are being supplied by eighteen supply nodes: terminals, refineries, and reservoirs, which are entirely located outside of the Manhattan, either in the adjacent boroughs or in the State of New Jersey. Supply and demand nodes are connected through the existing transportation network containing inner-city corridors, interstate highways, and twelve bridges which are the main points of entry to Manhattan (Omer et al., 2011). Figure 6 shows the case study layered in 2,475 sq. mile area including 29 demand nodes, 18

supply nodes, 685 transshipment nodes, and 2,103 transportation links. Aside covering the interstate highways and arterial which are used in the daily assignment of the fuel routing tasks, the case study area is further stretched out to enclose the distant transportation links which are located in non-vulnerable areas. This assures the model accuracy by inclusion of functional links that might be assigned to the fuel re-routing task in time of disaster.

To draw the transportation network, we extracted data from ArcGIS geodatabase (i.e. the 'native data structure' of ArcGIS). To do so, an application program interface (API) was planted in the Visual Basic (VB) environment to extract data from ESRI geodatabase and translate them to a graph network consisting of nodes and connecting arcs.

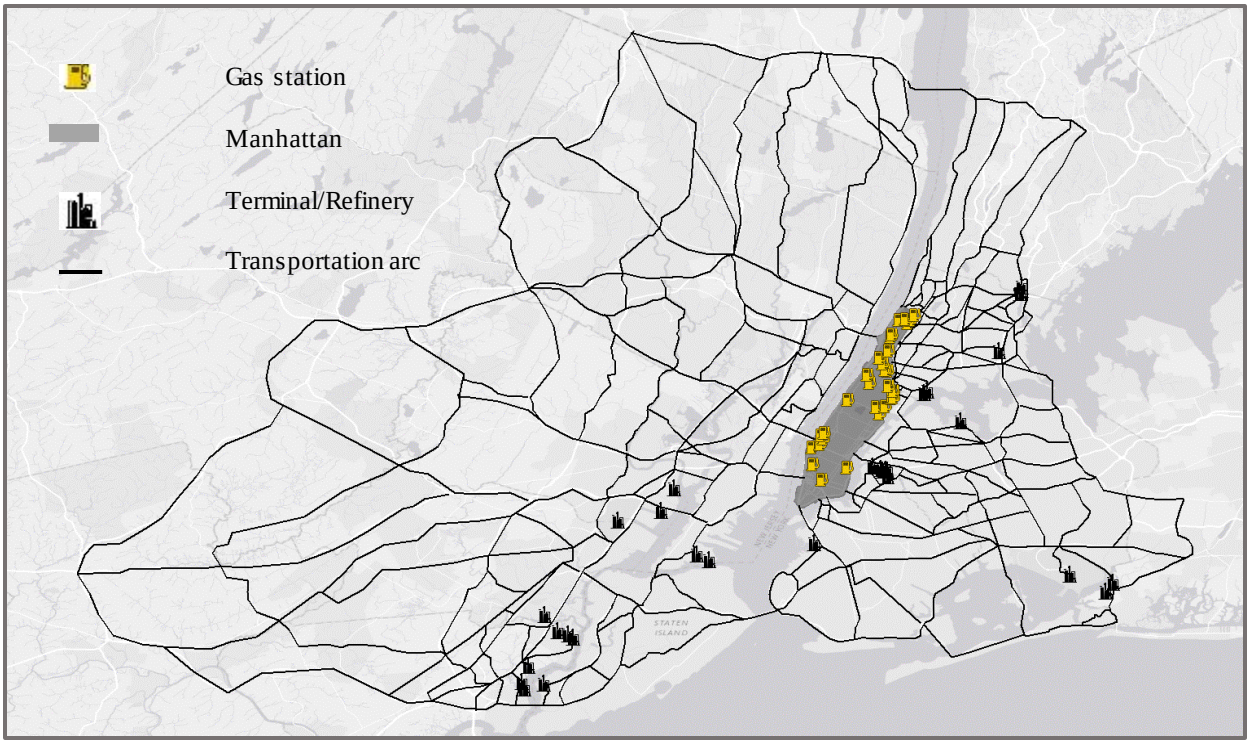

Figure 6. Manhattan's FSC

2.3.2. Modeling the FSC's inoperability in the aftermath of weather episodes

Modeling hurricanes aftermaths on Manhattan's FSC requires us to study the threats in three pillars of i) type and frequency, ii) vulnerable locations, and iii) expected flooding intensity.

2.3.2.1.Type and frequency of hurricanes

The Saffir-Simpson hurricane wind scale (SSHWS), provided by the U.S. National Hurricane Center (NHC), classifies hurricanes into five categories distinguished by the intensities of their sustained wind speeds. The return period of hurricanes categories is also modeled by NHC probability models. Table 3 summarizes further details on hurricanes' arrival chance in a given day within the Atlantic hurricane season (June 1 to November 30), as well as the sustained wind intensity corresponding to every category of hurricane.

Table 3. Scenarios' occurrence chance

Event	Description	Daily occurrence chance (%)	Sustained winds (mph)	Typical Characteristics	
				Surge (feet)	Damage[6]
1	No extreme event (BAU)	99.884	≤74[7]	-	-
2	Hurricane category 1	0.0258	74-95	4-5	Minimal
3	Hurricane category 2	0.0133	96-110	6-8	Moderate
4	Hurricane category 3	0.096[8]	111-129	9-12	Extensive
5	Hurricane category 4	0.0039	130-156[9]	13-18	Extreme

2.3.2.2.Vulnerable locations

Adapted from the National Oceanic and Atmospheric Administration's Sea, Lake, and Overland Surges from Hurricanes (SLOSH) model of New York City[10], Figure 7 shows the case study area's vulnerability to different categories of hurricane. In this figure, each of the four color-coded areas represents the potential zones which are subject to surge inundation in every category of hurricane.

[6] National Oceanic and Atmospheric Administration (NOAA): Technical Memorandum NWS TPC-5 (Blake et al. 2007)

[7] To be classified as a hurricane, a tropical cyclone must have maximum sustained winds of at least 74 mph (SSHWS).

[8] Responding to Climate Change in New York State: The ClimAID Integrated Assessment for Effective Climate Change Adaptation in New York State (ClimAID), http://www.nyserda.ny.gov/climaid

[9] According to the 2014 HMP, 'category 5 hurricane is not expected to occur in the New York City area because such a storm is not meteorologically sustainable north of Virginia'.

[10] http://gis.ny.gov/gisdata/inventories/details.cfm?DSID=1260

2.3.2.3.Expected intensity

In addition to vulnerability areas associating to hurricane categories, it's required to estimate the intensity of storm surge-induced flooding following each of the hurricane categories. Using the National Hurricane Center's 2010's SLOSH Maximum of the Maximum[11] Envelope of Water (MEOW) at high tide, the U.S. Army Corps of Engineers expects hurricanes' surge inundation depths, as shown in Figure 8.

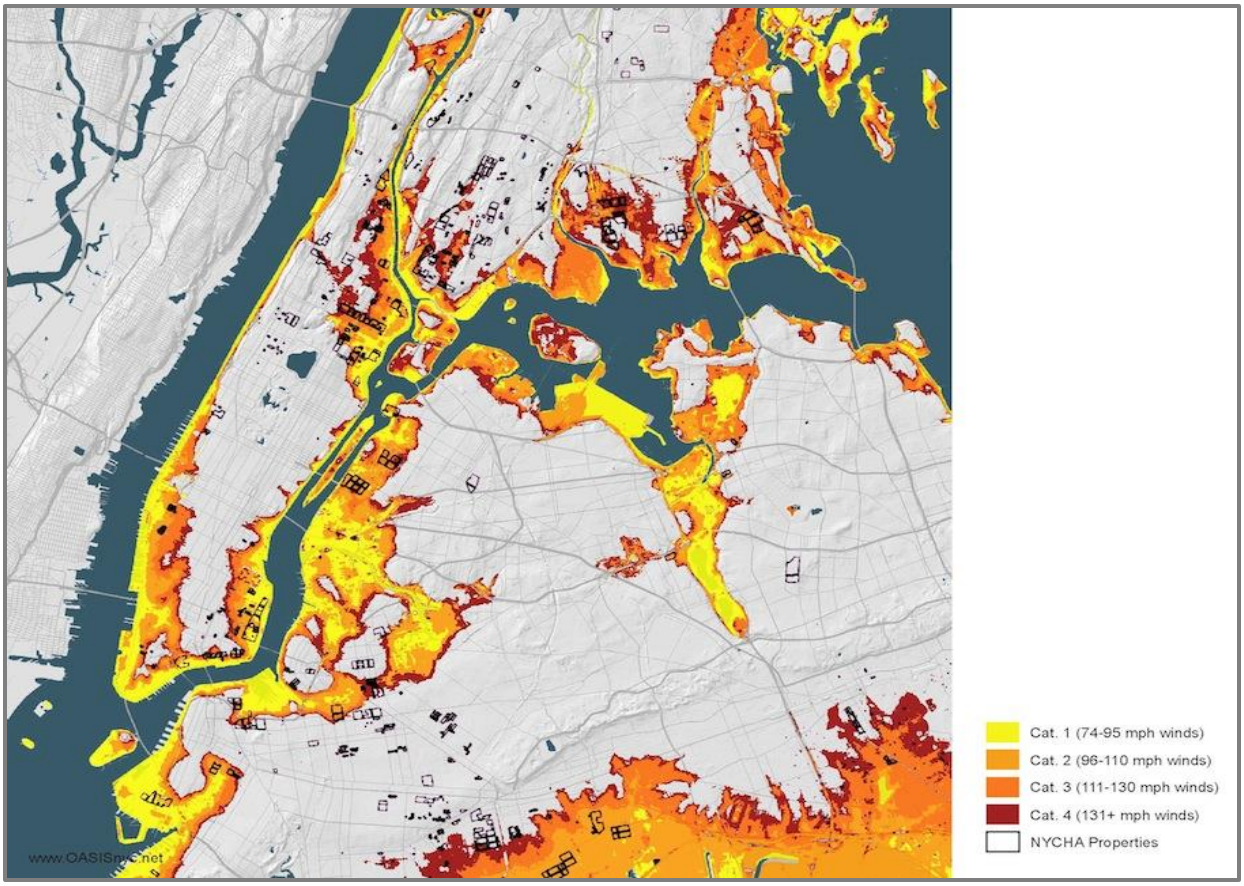

Figure 7. Hurricane corresponding vulnerable zones by category; Source: 2014 HMP

[11] SLOSH MOM

The estimated ocean-level surge height derived from the SLOSH MOM specifies the worst case surge height a given location may experience following a category of storm[12] 'based on thousands of possible storm scenarios at high tide.[13]'

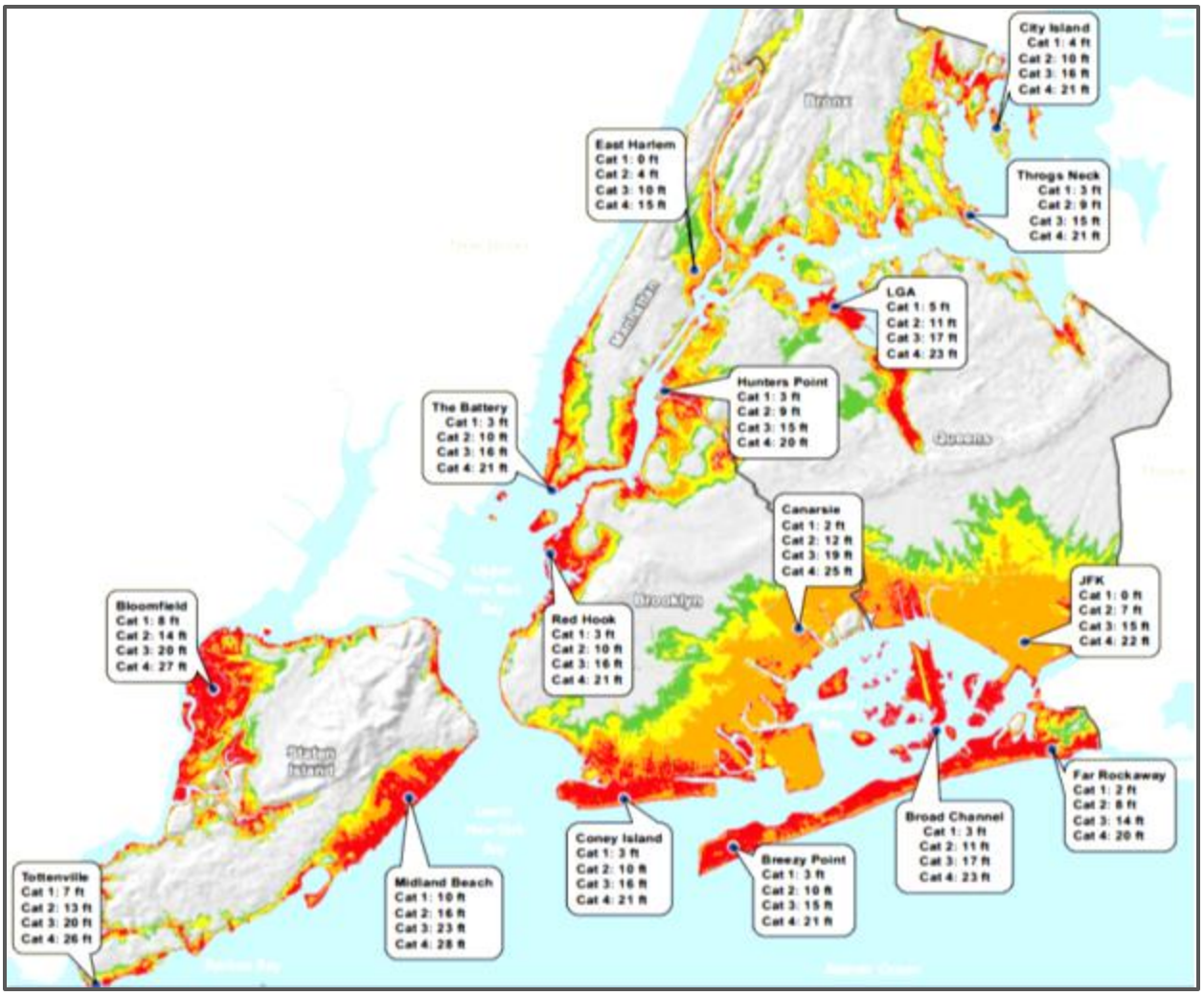

Figure 8. Expected inundation depth indicates a given location's worst case surge height; Source: 2014 HMP

As shown in Figure 7 and Figure 8, Manhattan's FSC is vulnerable to four categories of hurricane ranging from category 1, with the lowest impact magnitude, to category 4 with the highest impact. During each of

[12] 'The SLOSH model does not account for additional flooding due to rain, river flow, breaking waves/wave run-up, or astronomical high tide.'
[13] 2014 HMP

these categories, the infrastructure's elements perform differently. Precisely, a given element might be interrupted by a particular category of hurricane, if the element is i) located within the hurricane's corresponding flooding zone, and ii) vulnerable to the level of impact such one category may impose. The first condition, location of the FSC's elements, is investigated through projecting the geographical vulnerability zones (Figure 7) into the network of FSC discussed earlier. As shown, the NYC SLOSH model locates vulnerable areas to flood inundation subject to each category of hurricanes. Projection of vulnerable zones into the physical infrastructure network provides us with a map identifying those elements sited in every category of hurricane's flooding zones.

Practicing the second condition, however, requires one to study the threshold level of each element's operability and identify whether the modeled surge height exceeds the threshold level. Although few modeling tools are developed to estimate the hurricane damage, they all examine the damage to residential buildings. In absence of the information estimating the elements' robustness in the face of the storm surge, we assume the system's elements are fully vulnerable to hurricanes' aftermath. Meaning in case of hurricane category *n*, the FSC's elements which are sited in the vulnerability zones corresponding to the hurricane category *n* fail, no matter what surge elevation and wind intensity are expected for the coordination of the elements.

2.3.3. Resilience-enhancing strategies

Herein, we propose a set of candidate strategies to protect or otherwise, maintain the network's functionality in time of flooding. To do so, a line of resilience-enhancing strategies is developed for each type of the FSC's elements (fueling stations, terminals, transportation arcs, and transshipment nodes). To develop the list of RES, we reviewed the planning drafts, initiatives, and technical reports[14] which have addressed the

[14] These documents have been mainly prepared by either the City/State or foundations and institutional NGOs. While a majority of in-hand drafts discusses the issue in the policy domain, the technical documents which have developed analytical technics are very few in number. The later class of studies (mostly academic studies), focuses on a limited number of case studies, and to our knowledge, there is no technical article/report that models the fueling network of the NYC. Following documents represent a part of the efforts have been made by government and NGOs to address the NYC's disaster preparedness (resilience) planning:

- New York State Transportation Fuels Infrastructure Study (2014)

NYC's flood resilient infrastructures. Table 4 categorizes these strategies in three pillars of absorptive- (to maintain elements capabilities to withstand the hurricanes aftermath), adaptive- (to provide disrupted elements with an alternative method to perform), and restorative-enhancing strategies (to ease the recovery process).

http://www.nyserda.ny.gov/About/Publications/EA-Reports-and-Studies/Petroleum-Infrastructure-Studies

- The City of New York Hazard Mitigation Plan (2015) http://www1.nyc.gov/site/em/ready/hazard-mitigation.page
- A Stronger, More Resilient New York (2013) http://www.nyc.gov/html/sirr/html/report/report.shtml
- One New York - The Plan for a Strong and Just City (2015) http://www.nyc.gov/html/onenyc/downloads/pdf/publications/OneNYC.pdf
- New York Panel on Climate Change Report (2015) http://onlinelibrary.wiley.com/doi/10.1111/nyas.2015.1336.issue-1/issuetoc
- PlaNYC Progress Report (2014) http://www.nyc.gov/html/planyc2030/downloads/pdf/140422_PlaNYCP-Report_FINAL_Web.pdf
- One City Built to Last (2015), http://www.nyc.gov/html/builttolast/assets/downloads/pdf/OneCity.pdf
- NYC Recovery: The New York City Community Development Block Grant Disaster Recovery (CDBG-DR) Action Plan (2016) http://www.nyc.gov/html/cdbg/downloads/pdf/cdbg-dr_action_plan_incorporating_amendments_1-11.pdf
- Post-Sandy Initiative (2013) http://postsandyinitiative.org/wp-content/uploads/2013/05/Post-Sandy-Report_Full.pdf
- Hurricane Sandy Rebuilding Strategy (2013) http://portal.hud.gov/hudportal/documents/huddoc?id=HSRebuildingStrategy.pdf
- North Atlantic Coast Comprehensive Study (NACCS), Emergency Costs (2015) http://www.nad.usace.army.mil/Portals/40/docs/NACCS/10B_Emergency_Costs_26Jan2015.pdf
- NYS 2100 Commission report (2012) https://www.google.com/webhp?sourceid=chrome-instant&ion=1&espv=2&ie=UTF-8#q=%E2%80%A2+NYS+2100+Commission+report

Table 4. Resilience-enhancing Strategies

Resilience-enhancing strategies

Capacity Enhancing Strategies	FSC's elements				Strategy's goal	Cost in $ ($\times 10^3$)
	Gas stations	Terminals	Arcs	Transshipment Nodes		
Absorption	Protective roofing and reinforced canopies[15], elevated electric devices, drainage improvements, deployable floodwalls and sandbags[16], sealed electric system[17], water pumps, and shatter-resistant operable windows and frames.				Protecting against hurricane cat. 1	17
					Protecting against hurricane cat. 2	25
					Protecting against hurricane cat. 3	25
					Protecting against hurricane cat. 4	40
		Hardening exposed shorelines with armor stone and constructing levee, rip-rap[18], floodwalls, and bulkheads16. Backflow-prevention devices, drainage improvements, elevated critical buildings, and			Protecting against hurricane cat. 1	7,000
					Protecting against hurricane cat. 2	12,000
					Protecting against hurricane cat. 3	20,000

[15] Improvement Center (http://www.improvementcenter.com/roofing/3-roofing-materials-that-can-survive-high-winds.html)
[16] James 2010; Tsvetanov et al. 2013; Tsvetanov et al. 2012; Aerts et al. 2013
[17] FEMA Restoring Mechanical, Electrical, and Plumbing Systems In Non-Substantially Damaged Residential Buildings (2013)
[18] Flood Mitigation Engineering Resource Center (FMERC) – Project EC14-005 (2014)

		drainage improvements. Sealed electric system[19]. Elevated onsite tanks and relocated critical facilities[20].			Protecting against hurricane cat. 4	20,000
			Flood-proofed bridge21 and tunnels[21], raised street stocking level18. Removed asphalt with natural or synthetic turf, new drainage systems18, and tree pruning.		Protecting against hurricane cat. 1	120
					Protecting against hurricane cat. 2	180
					Protecting against hurricane cat. 3	250
					Protecting against hurricane cat. 4	400
Adaptation	Backup generator and switching key[22].				Protecting against hurricane cat. 1	25
					Protecting against hurricane cat. 2	25
					Protecting against hurricane cat. 3	25
					Protecting against hurricane cat. 4	25
		Standby emergency generators, backup			Protecting against hurricane cat. 1	7,000

[19] The Association for Convenience & Fuel Retailing (NACS), Fuel Reports (2013)

[20] ICF International, New York State Petroleum Terminal Resiliency Assessment NYSERDA Contract 30186 (2014)

[21] North Atlantic Coast Comprehensive Study (NACCS) Emergency Costs (2015)

[22] NYS Energy Research and Development Authority, PON 2758 Administrator

		facilities20 for refining process and on site reservoir tanks for crude oil23.			Protecting against hurricane cat. 2	7,000
					Protecting against hurricane cat. 3	7,000
					Protecting against hurricane cat. 4	7,000
Restoration				Reservoir tanks in four designated locations: The Bronx, Brooklyn, Staten Island, and New Jersey, each in three capacities[23].	0.5 million gallons	5,000
					1 million gallons	7,500
					3 million gallons	10,000

[23] NYS Governor Announcement (2014)
https://www.governor.ny.gov/news/governor-cuomo-announces-broad-series-innovative-protections-vice-president-biden-credits#

As shown in table 4, each type of the network's elements is matched with at least one category of the RES. For example, there are two lines of strategies available to improve the gas stations' resilience: (1) strategies to enhance the stations' absorptive capacity and (2) strategies to increase the stations' adoptive capacity. The former line of strategies is developed to assist fueling stations in better absorbing the hurricanes' aftermath. In fact, this happens through the improvement of the stations' physical structure to better withstand the hurricanes' direct impacts including storm surge and wind. The absorptive strategies for gas stations range from protective roofing, reinforced canopies, and shatter-resistant operable windows (protection against wind) to drainage improvements, deployable floodwalls and sandbags, and sealed electric systems (protection against surge). The latter type of the strategies, yet enhances the stations' capacity to better cope with the indirect effects of hurricanes which are rippled by interdependent infrastructures such as power grid. In the case of a power outage, as an example of indirect failure, equipment such as backup generators and switching keys assist gas stations to adopt with the existing inoperability.

In total, six lines (packages) of strategies are available to enhance the system's resilience: absorption strategies for the gas stations, terminals, and transportation arcs; adaptation strategies for the gas stations and terminals; and an investment-package of restoration strategies for the transshipment nodes. To this end, we made two assumptions.

First, every package of the RES (with the exception of the recovery package) could be tailored for a given category of hurricane. Meaning that within every package, there are 4 capacity-enhancing levels (investment level), each corresponds to a category of hurricane. Meaning, to protect a given element against a particular hurricane of category n, it is required to invest on the corresponding investment-package with the level of capacity-enhancing equal or larger n. If no package or a package with a capacity-enhancing level smaller than n is chosen, the investment would be ineffective and the element of interest remains fully-vulnerable against the hurricane category n. Otherwise, the element becomes robust against any hurricane with the category equal or lower n. Second, there is a corresponding cost to each investment-package and

to every enhancing level within a package. By elevating the package's enhancing level, the corresponding cost increases. The very last column of table 4 assumes the investment cost in dollar value for every enhancing level of each of the investment-packages. The matching costs are extracted from existing reports and acts which are led by the NYC and the State (reports are addressed through the footnote of the table 4).

2.4. Model formulation

2.4.1. General Structure

In this section, we propose a mathematical model to maximize the FSC's resilience given: i) random arrival and characteristics of extreme events, ii) network's inherent capacity to withstand and possibly cope with the imposed shocks, iii) strategies available to enhance the system's overall resilience, and iv) inevitable budgeting and technological restrictions. In theory, while the FSC's functionality is vulnerable to sever weather episodes, it could be protected and possibly enhanced by a set of strategies put in place before a given hazard attacks the system. This means the FSC's post-event behavior (fuel distribution) is conditioned on pre-event decisions (RES). Accordingly, we split the decision variables into two stages. The first stage variables include pre-event decisions allocating resources on different packages of RES and on different elements of the FSC. The second stage variables include the decisions on the fuel distribution/routing assignment in which the system experiences the maximum operability. The randomness embedded in the arrival of events combined with the separation of the pre-event investments and post-event fuel replenishment assignments leads the model formulation to a bi-stage stochastic framework.

To show the general structure of the proposed model, we represent the FSC as a directed graph G (O, A); where O is a set of nodes with three subsets of supply nodes, demand nodes, and transshipment nodes (nodes with no supply and no demand), and A is a set of arcs connecting nodes. The general model formulation is shown in Figure 9.

$$\text{Min} \quad \sum_{n=1}^{N} \mathbb{P}_n [\, \mathrm{E}(\sum_{d=1}^{D} U_{d,n} / No(d)) + C_n X_n] \tag{2.1}$$

$$\text{s.t.} \quad \mathbb{V} = \Lambda(\alpha, \beta, \rho, n) \qquad \forall \alpha, \beta, \rho, n \tag{2.2}$$

$$\mathbb{V} \leq \mathbb{B} \tag{2.3}$$

$$f(\boldsymbol{\alpha}, \beta, \rho, n) \geq X(\beta, n) \qquad \forall\, \boldsymbol{\alpha}, \beta, \rho, n \tag{2.4}$$

$$\sum_{o'}^{O'} X(o, o', n) - \sum_{o'}^{O'} X(o', o, n) = F_{o,n} \qquad \forall\, d, t, n \tag{2.5}$$

$$X(\beta, n) \leq \mathrm{W}(n) \qquad \forall\, \beta, n \tag{2.6}$$

$$I_{\mathrm{n}}(\alpha, \beta, \rho) \in \mathrm{I} \qquad \forall\, \boldsymbol{\alpha}, \beta, \rho, n \tag{2.7}$$

Figure 9. General model formulation

The proposed system's resilience index is averaged met-demand across the gas stations. To this end, we define a variable representing the unmet-demand rate (UDR) and solve the model for the minimum expected value of the UDR (i.e. maximum resilience). The objective function, Equation (2.1), includes two parts: (i) the expected UDR of gas station d, during scenario n, indicated as $U_{d,n}$, averaged across all demand nodes, and (ii) the fuel distribution cost, $C_n X_n$, where C_n represents unit distribution cost and X_n denotes distributed flow during scenario n. Both parts are weighted across the occurrence probability associated with scenario n, $\mathbb{P}_n$.

Constraint (2.2) elaborates the breakdown of the pre-event investment cost, $\mathbb{V}$, covering the total dollar values required to invest on those packages of the RES which are chosen by the solution to the model ($\boldsymbol{\alpha}$, β, and ρ indicating adaptive-, absorptive-, and restorative-enhancing strategies, respectively). Constraint (2.3) caps the investment costs $\mathbb{V}$ under available budget $\mathbb{B}$. Constraints (2.4) and (2.5) reflect flow conservation restrictions. Constraint (2.4) governs that a given node is operable during scenario n, if the node and its outgoing arcs are not disturbed by scenario n, or if they are, the corresponding packages of the RES are implemented to maintain the operability of the node and its outgoing arcs. Constraint (2.5) assures the balance of outgoing and incoming flows meets the given node's supply/demand rate. Constraint (2.6), the flow capacity constraint, conditions the functionality of the disturbed arcs on investment on the corresponding packages of the RES and bounds the transshipping flows under the links capacity W.

Constraint (2.7) ensures that investment packages are chosen from the assumed set of RES provided in Table 4. At the end, the proposed model performs a simultaneous search on a bundle of pre-event investment packages and post-event fuel distribution patterns yielding the maximum resilience.

2.4.2. Resilience-enhancing model

Notations employed through this section are synopsized in Table 5.

Table 5. Nomenclature

Sets	
$\{n\} = \{1, 2, ..., N\}$	Scenarios
$\{\alpha\} = \{1, 2, ..., A\}$	Adaptive-enhancing packages
$\{\beta\} = \{1, 2, ..., B\}$	Absorptive-enhancing package
$\{\rho\} = \{1, 2, ..., P\}$	Restorative-enhancing package
$\{s\} = \{1, 2, ..., S\}$	Supply nodes (terminals)
$\{t\} = \{1, 2, ..., T\}$	Transshipment nodes (t' for alias)
$\{d\} = \{1,2, ..., D\}$	Demand nodes (gas stations)
$\{k\} = \{1,2, ..., K\}$	Fuel types[24]
Parameters	
$\mathbb{L}$	A sufficiently large number ($\mathbb{L} \gg \mathbb{B}$)
$\mathbb{B}$	Total budget available for the RES
ε	A small positive infinitesimal quantity
$\mathbb{P}_n$	Occurrence probability of scenario n
$F_{d,n}^{k}$	Demand of commodity k in demand node d, during scenario n
$F_{s,n}^{k}$	Supply of commodity k in supply node s, during scenario n
$F_{t,n}^{k}$	Demand of commodity k in transshipment node t, during scenario n
$No(d^k)$	Number of demand nodes (gas stations) of commodity k in Manhattan

[24] The proposed model is developed base on a single type of fuel: gasoline. However, the model could be extended to the multi-commodity form.

$C^{k}_{s,t,n}$ Distance between supply node *s* and transshipment node *t*, during scenario *n*

$C^{k}_{t,t\prime,n}$ Distance between two transshipment nodes, during scenario *n*

$C^{k}_{t,d,n}$ Distance between transshipment node *t* and demand node *d*, during scenario *n*

$V^{k,\beta}_{s}$ Cost of absorptive-enhancing package β for supply node *s*

$V^{k,\beta}_{d}$ Cost of absorptive-enhancing package β for demand node *d*

$V^{\beta}_{s,t}$ Cost of absorptive-enhancing package β for the arc connecting *s* to *t*

$V^{\beta}_{t,t\prime}$ Cost of absorptive-enhancing package β for transshipment arc

$V^{\beta}_{t,d}$ Cost of absorptive-enhancing package β for the arc connecting *t* to *d*

$V^{k,\alpha}_{s}$ Cost of adaptive-enhancing package α for supply node *s*

$V^{k,\alpha}_{d}$ Cost of adaptive-enhancing package α for demand node *d*

$V^{k,\rho}_{t}$ Cost of restorative strategy ρ for transshipment node *t*

$O^{k}_{s,n}$ Dummy indicator: Operability of node *s* during scenario *n*. 1 if operable, 0 otherwise.

$O^{k}_{d,n}$ Dummy indicator: Operability of node *d* during scenario *n*. 1 if operable, 0 otherwise.

$O_{s,t,n}$ Dummy indicator: Operability of arc (*s*,*t*) during scenario *n*. 1 if operable, 0 otherwise.

$O_{t,t\prime,n}$ Dummy indicator: Operability of transshipment arc during scenario *n*. 1 if operable, 0 otherwise.

$O_{t,d,n}$ Dummy indicator: Operability of arc (*t*,*d*) during scenario *n*. 1 if operable, 0 otherwise.

E_{α} Corresponding parameter to the enhancing level of the adaptive-enhancing package α (the highest category of hurricane that this package can handle), range 1 to 4

E_{n} Corresponding parameter to the scenario *n* (category of hurricane corresponding to the scenario *n*), ranged 1 to 4

E_{β} Corresponding parameter to the enhancing level of the absorptive-enhancing package β (the highest category of hurricane that this package can handle), ranged 1 to 4

$RTC^{k,\rho}_{t}$ Capacity of the reservoir tank proposed by the restorative strategy ρ in node *t*, corresponding to fuel type *k*

$W_{s,t,n}$ Nominal capacity of arc (s, *t*), during scenario *n*

$W_{t,t\prime,n}$ Nominal capacity of the transshipment arc, during scenario *n*

$W_{t,d,n}$ Nominal capacity of arc (*t*, *d*), during scenario *n*

$BL_{t,t\prime}$	Dummy indicator for identifying the bridges. 1 if arc (t, t') is a bridge, 0 otherwise.

Decision variables

$U_{d,n}^{k}$	UDR corresponding to fuel type k, in demand node d, during scenario n
$X_{s,t,n}^{k}$	Flow type k on arc (s,t), during scenario n
$X_{t,t\prime,n}^{k}$	Flow type k on transshipment arc, during scenario n
$X_{t,d,n}^{k}$	Flow type k on arc (s,d), during scenario n
$\mathbb{V}$	The implementation cost of the resilience-enhancing packages chosen by the model
$I_{s}^{k,\beta}$	Binary variable; 1 if absorptive-enhancing package β is chosen for facilities corresponding to fuel type k at supply node s, 0 otherwise.
$I_{d}^{k,\beta}$	Binary variable; 1 if absorptive-enhancing package β is chosen for facilities corresponding to fuel type k at demand node d, 0 otherwise.
$I_{s,t}^{\beta}$	Binary variable; 1 if absorptive-enhancing package β is chosen for arc (s,t), 0 otherwise.
$I_{t,t\prime}^{\beta}$	Binary variable; 1 if absorptive-enhancing package β is chosen for transshipment arc, 0 otherwise.
$I_{t,d}^{\beta}$	Binary variable; 1 if absorptive-enhancing package β is chosen for arc (t,d), 0 otherwise.
$I_{s}^{k,\alpha}$	Binary variable; 1 if adaptive-enhancing package α is chosen for facilities corresponding to fuel type k in supply node s, 0 otherwise.
$I_{d}^{k,\alpha}$	Binary variable; 1 if adaptive-enhancing package α is chosen for facilities corresponding to fuel type k in demand node d, 0 otherwise.
$I_{t}^{k,\rho}$	Binary variable; 1 if restorative strategy ρ is chosen for facilities corresponding to fuel type k in node t, 0 otherwise.

Figure 10 shows an extension to the framework discussed in Section 2.4.1.

$$Min \quad \sum_{n=1}^{N} \mathbb{P}_n \left[\mathbb{L} \frac{\sum_{d=1}^{D} \sum_{k=1}^{K} U_{d,n}^{k}}{\sum_{k=1}^{K} NO(d^k)} + \sum_{s=1}^{S} \sum_{t=1}^{T} \sum_{k=1}^{K} X_{s,t,n}^{k} C_{s,t,n}^{k} + \sum_{t=1}^{T} \sum_{t\prime=1}^{T\prime} \sum_{k=1}^{K} X_{t,t\prime,n}^{k} C_{t,t\prime,n}^{k} + \sum_{t=1}^{T} \sum_{d=1}^{D} \sum_{k=1}^{K} X_{t,d,n}^{k} C_{t,d,n}^{k} \right] + \mathbb{V} \tag{2.8}$$

$$s.t. \quad \mathbb{V} = \sum_{\beta=1}^{B} \left(\sum_{s=1}^{S} \sum_{k=1}^{K} I_{s}^{k,\beta} V_{s}^{k,\beta} + \sum_{d=1}^{D} \sum_{k=1}^{K} I_{d}^{k,\beta} V_{d}^{k,\beta} + \sum_{s=1}^{S} \sum_{t=1}^{T} I_{s,t}^{\beta} V_{s,t}^{\beta} + \sum_{t=1}^{T} \sum_{t\prime=1}^{T\prime} I_{t,t\prime}^{\beta} V_{t,t\prime}^{\beta} BL_{t,t\prime} + \sum_{t=1}^{T} \sum_{d=1}^{D} I_{t,d}^{\beta} V_{t,d}^{\beta} \right) + \sum_{\alpha=1}^{A} \sum_{k=1}^{K} \left(\sum_{s=1}^{S} I_{s}^{k,\alpha} V_{s}^{k,\alpha} + \sum_{d=1}^{D} I_{d}^{k,\alpha} V_{d}^{k,\alpha} \right) + \sum_{\rho=1}^{P} \sum_{t=1}^{T} \sum_{k=1}^{K} I_{t}^{k,\rho} V_{t}^{k,\rho} \tag{2.9}$$

$$\mathbb{V} \leq \mathbb{B} \tag{2.10}$$

$$U^k_{d,n} = (F^k_{d,n} - \sum_{t=1}^{T} X^k_{t,d,n}) \,/\, F^k_{d,n} \tag{2.11}$$

$$F^k_{s,n}[O^k_{s,n} + ((1 - O^k_{s,n})(\sum_{\alpha=1}^{A} I^{k,\alpha}_s \lceil [(E_\alpha - E_n)/\max\{E_\alpha - E_n\}] + \varepsilon \rceil)) \\ (\sum_{\beta=1}^{B} I^{k,\beta}_s \lceil [(E_\beta - E_n)/max\{E_\beta - E_n\}] + \varepsilon \rceil))] \geq \sum_{t=1}^{T} X^k_{s,t,n} \qquad \forall\, s, n, k \tag{2.12}$$

$$F^k_{d,n}[O^k_{d,n} + ((1 - O^k_{d,n})(\sum_{\alpha=1}^{A} I^{k,\alpha}_s \lceil [(E_\alpha - E_n)/\max\{E_\alpha - E_n\}] + \varepsilon \rceil)) \\ (\sum_{\beta=1}^{B} I^{k,\beta}_d \lceil [(E_\beta - E_n)/max\{E_\beta - E_n\}] + \varepsilon \rceil))] \geq \sum_{t=1}^{T} X^k_{t,d,n} \qquad \forall\, d, n, k \tag{2.13}$$

$$F^k_{t,n} + \sum_{\rho=1}^{P} RTC^{k,\rho}_t \, I^{k,\rho}_t \geq \sum_{d=1}^{D} X^k_{t,d,n} + \sum_{t'=1}^{T'} X^k_{t,t',n} - \sum_{d=1}^{D} X^k_{s,t,n} - \sum_{t'=1}^{T'} X^k_{t',t,n} \quad \forall\, t, n, k \tag{2.14}$$

$$\sum_{k=1}^{K} X^k_{s,t,n} \leq W_{s,t,n}[O_{s,t,n} + ((1 - O_{s,t,n})(\sum_{\beta=1}^{B} I^{\beta}_{s,t} \lceil [(E_\beta - E_n)/\max\{E_\beta - E_n\}] + \varepsilon \rceil))] \qquad \forall\, s, t, n \tag{2.15}$$

$$\sum_{k=1}^{K} X^k_{t,t',n} \leq W_{t,t',n}[O_{t,t',n} + ((1 - O_{t,t',n})(\sum_{\beta=1}^{B} I^{\beta}_{t,t'} \lceil [(E_\beta - E_n)/\max\{E_\beta - E_n\}] + \varepsilon \rceil))] \qquad \forall\, t, t', n \tag{2.16}$$

$$\sum_{k=1}^{K} X^k_{t,d,n} \leq W_{t,d,n}[O_{t,d,n} + ((1 - O_{t,d,n})(\sum_{\beta=1}^{B} I^{\beta}_{t,d} \lceil [(E_\beta - E_n)/\max\{E_\beta - E_n\}] + \varepsilon \rceil))] \qquad \forall\, s, t, n \tag{2.17}$$

$$\sum_{\rho=1}^{P} I^{k,\rho}_t \leq 1 \qquad \forall\, k, t \tag{2.18}$$

$$\sum_{\beta=1}^{B} I^{k,\beta}_s \leq 1 \qquad \forall\, k, s \tag{2.19}$$

$$\sum_{\alpha=1}^{A} I^{k,\alpha}_s \leq 1 \qquad \forall\, k, s \tag{2.20}$$

$$\sum_{\alpha=1}^{A} I^{k,\alpha}_d \leq 1 \qquad \forall\, k, d \tag{2.21}$$

$$\sum_{\beta=1}^{B} I^{k,\beta}_d \leq 1 \qquad \forall\, k, d \tag{2.22}$$

$$\sum_{\beta=1}^{B} I^{\beta}_{s,t} \leq 1 \qquad \forall\, s, t \tag{2.23}$$

$$\sum_{\beta=1}^{B} I^{\beta}_{t,t'} \leq 1 \qquad \forall\, t, t' \tag{2.24}$$

$$\sum_{\beta=1}^{B} I^{\beta}_{t,d} \leq 1 \qquad \forall\, t, d \tag{2.25}$$

$$X^k_{s,t,n} \geq 0 \qquad \forall\, k, s, t, n \tag{2.26}$$

$$X^{k}_{t,t',n} \geq 0 \qquad \forall\, k, t, t', n \qquad (2.27)$$

$$X^{k}_{t,d,n} \geq 0 \qquad \forall\, k, t, d, n \qquad (2.28)$$

Figure 10. Model Formulation

The primary goal of this model is to minimize the FSC's overall inoperability (UDR) and the secondary goal is to minimize the fuel distribution cost. Consequently, the objective, Equation (2.8), minimizes the expected UDR and fuel distribution cost over all scenarios. Both values are weighted over the occurrence probabilities of the events. Within the objective function, two factors are embedded: i) scalar $\mathbb{L}$, as a sufficiently large number, which prioritizes the least expected UDR over the fuel distribution cost and ii) variable $\mathbb{V}$ (costs of the resilience-enhancing packages chosen by the model) which protects the budget against unnecessary expenses having no impact on the resilience index.

Constraint (2.9) captures the dollar value associated with implementation of the selected resilience-enhancing packages (the cost of decisions made in the first stage). Constraint (2.10) limits the cost of the proposed strategies under the project's budget. Constraint (2.11) represents the inoperability index (UDR) which is equal to the ratio of unsatisfied demand to expected demand, averaged over all gas stations. Constraints (2.12) -(2.14) indicate flow conservations in terminals, gas stations, and transshipment nodes. Constraint (2.12) shows that a given terminal's outgoing flow is upper-bounded by the terminal's available supply. This constraint also conditions the operability of a given terminal, *s*, on the following condition: if a given terminal is off the vulnerability areas of the hurricane category *n*, it remains operable; otherwise, the corresponding absorptive- and adaptive-enhancing packages must be implemented to maintain the functionality of the terminal against the aftermath expected in scenario *n*.

Within the constraint (2.12), the term $\lceil [(E_\alpha - E_n)/max\{E_\alpha - E_n\}] + \varepsilon \rceil$ is designed as a dummy variable, to assure the corresponding package that is chosen for operability of a particular terminal during scenario *n* should be able to handle the aftermath corresponding to the hurricane categories *n* and smaller than *n*. Constraints (2.13) and (2.14) embody the same concept for gas stations and transshipment nodes,

respectively. Here, we assume the inoperable terminals or gas stations become operable, if both absorption and adaptation strategies are chosen simultaneously.

This assumption, however, makes constraints (2.12) and (2.13) nonlinear. Constraints (2.15) -(2.17) govern the flow capacity of arcs and restrict distributed flows to the arcs' nominal capacities. Similar to the concept used in flow conservation constraints, a given arc's functionality in scenario *n* is conditioned on either robustness of that arc against the scenario *n*'s corresponding aftermath or implication of the absorptive-enhancing packages that can handle hurricanes categories *n* or larger.

Constraints (2.18) -(2.25) restrict the model to invest on at most one enhancing level of each type of the resilience-enhancing packages and for each network's element. For example, a given terminal cannot receive two series of absorptive-enhancing package related to hurricanes category 2 and category 4. If the level-four investment (which is tailored to protect the element against hurricane category 4) is granted, an investment in the level-two package is redundant and if the level-two package is picked, the given element remains vulnerable to hurricanes stronger than category 2. Finally, constraints (2.26) -(2.28) reassure the non-negativity of flows.

2.5. Computational experiments

To investigate the vulnerability of Manhattan's FSC against the extreme weather episodes and explore the impact of the RES on system's productivity, we set up a number of experiments and examined different policy scenarios, physical improvements, and budget limitations.

The first experiment investigates the FSC's resilience with no opportunity for capacity enhancement. In this experiment, the FSC is examined under five possible scenarios; BAU (when there is no extreme event threatening the network) and hurricane categories 1-4. However, experiments 2-4 investigate the FSC's functionality given investment on absorptive-, adoptive-, and restorative-enhancing packages, respectively. Table 6 illustrates the FSC's response to experiments 1-4.

Table 6. Metrics of experiments 1-4

Scenario number	Description	Available budget ($M)	RES Cost ($M)	Fuel supplied by terminals (gallon)	Average mile flowed by fuels from terminals to gas stations (mile)	UDR
Experiment 1						
No investment opportunity						
1	BAU	0	N/A	89,765	9.229	0
2	Hurricane cat. 1	0	N/A	51,202	11.839	0.504
3	Hurricane cat. 2	0	N/A	7,716	34.95	0.935
4	Hurricane cat. 3	0	N/A	0	0	1
5	Hurricane cat. 4	0	N/A	0	0	1
Experiment 2						
Investment on absorptive strategies						
1	Cat. 1-5	0	N/A	129,706	9.427	0.042
2	Cat. 1-5	0.5	0	129,706	9.427	0.042
3	Cat. 1-5	1	0	129,706	9.427	0.042
4	Cat. 1-5	2	1.242	129,942	10.315	0.041
5	Cat. 1-5	3	1.242	129,942	10.315	0.041
6	Cat. 1-5	4	1.242	129,942	10.315	0.041
7	Cat. 1-5	5	1.242	129,942	10.315	0.041
8	Cat. 1-5	6	1.242	129,942	10.315	0.041
9	Cat. 1-5	7	1.242	129,942	10.315	0.041
10	Cat. 1-5	8	6.936	133,108	10.12	0.04
11	Cat. 1-5	9	6.936	133,108	10.12	0.04
12	Cat. 1-5	10	6.936	133,108	10.12	0.04
13	Cat. 1-5	20	19.738	136,510	9.769	0.039
14	Cat. 1-5	50	19.738	136,510	9.763	0.039
15	Cat. 1-5	100	19.738	136,510	9.763	0.039
Experiment 3						

Investment on adaptive strategies						
1	Cat. 1-5	0	N/A	129,706	9.427	0.042
2	Cat. 1-5	10	0	129,706	9.427	0.042
3	Cat. 1-5	50	0	129,706	9.427	0.042
4	Cat. 1-5	100	0	129,706	9.427	0.042
Experiment 4						
Investment on restorative strategies						
1	Cat. 1-5	0	N/A	129,706	9.427	0.042
2	Cat. 1-5	5	5	41,744	25.400	0.011
3	Cat. 1-5	10	5	41,744	25.400	0.011
4	Cat. 1-5	15	5	41,744	17.369	0.011
5	Cat. 1-5	20	5	41,744	17.315	0.011
6	Cat. 1-5	30	5	41,744	17.313	0.011

Results of the experiments 2-4 are graphed in Figure 11

Experiment 2

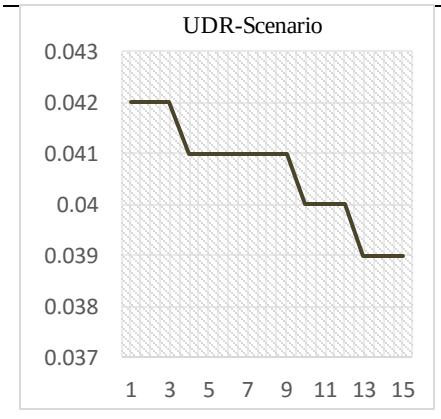

Figure 11.a

Experiment 3

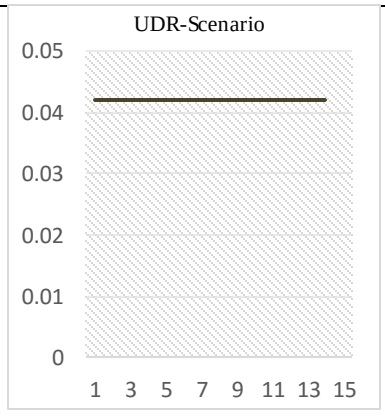

Figure 11.d

Experiment 4

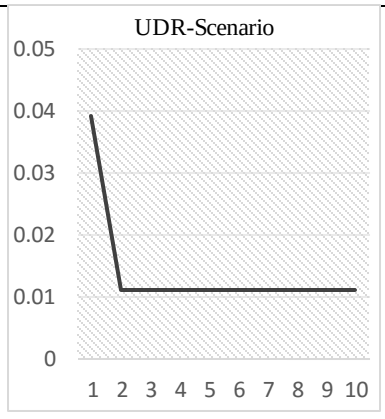

Figure 11.g

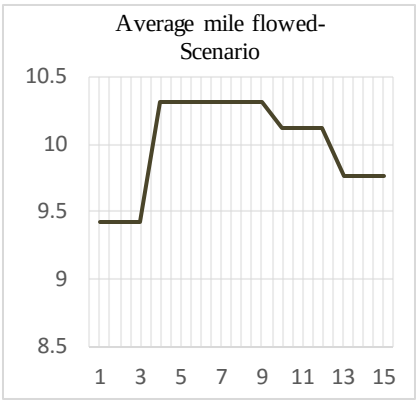

Figure 11.b

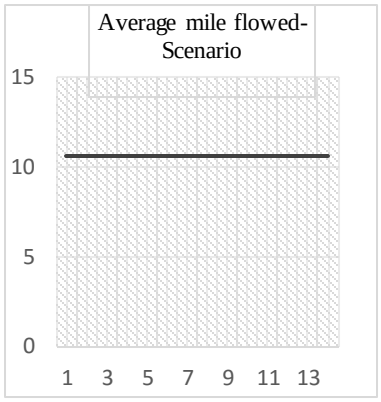

Figure 11.e

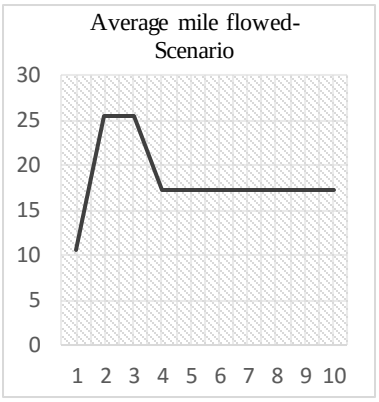

Figure 11.h

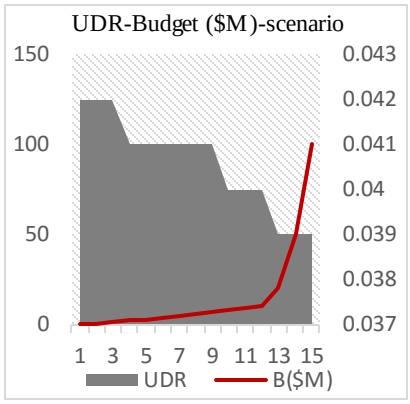

Figure 11.c

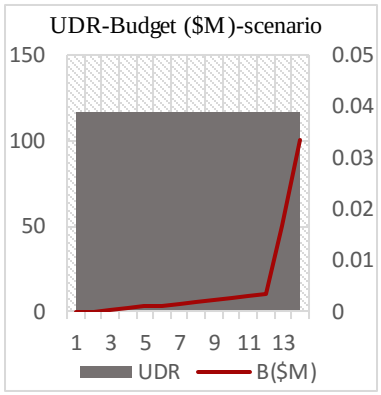

Figure 11.f

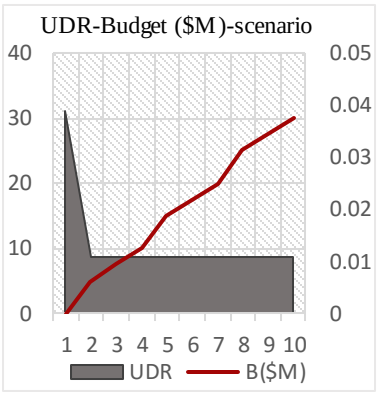

Figure 11.i

Figure 11. Results of the experiments 2-4

The first experiment shows the FSC's inherent capability in distributing fuel across the network. While there is no unmet demand in BAU, the FSC responds differently to each category of the hurricane. During hurricane categories 1 and 2, the FSC loses 50 and 93.5 percent of its resilience and during categories 3 and 4 becomes fully inoperable. By increasing the hurricane's intensity, the average mile flowed by fuel increases. In fact, fuel routing changes, since a greater number of arcs becomes inoperable under more severe weather episodes.

The last three experiments study the system's response to RES packages. As shown in Figure 11.a, absorptive packages, individually, have a limited impact on the system's overall resilience. The reason is the nonlinearity of constraints (2.12) and (2.13); where the network's elements are robust against a given

hurricane category, if both of the absorptive and adaptive packages are performed. Consequently, the absorptive strategies, solely, cannot maintain the functionality of the gas stations and terminals. Whereas, these strategies can maintain the functionality of the transportation network's arcs. Figure 11.c shows how maintained arcs drops the UDR, though the change is limited to 0.3%. In contrast to the absorptive packages, adaptive packages have no effect on the system's resilience.

As explained, in absence of absorptive strategies, adaptive strategies, individually, have no influence on elements' robustness. Figures 11.d-11.f show how the FSC remains non-responsive to investment options on adaptive strategies. In comparison to the first two packages of RES, restorative strategies escalate the system's resilience significantly. As shown in figure 11.g-11.i (experiment 4), dysfunctional elements lead the infrastructures towards partial operability. In response, the model invests on reservoir tank(s) to bypass the terminals which are located in valuable areas. In the other word, since the experiment restricts the model to invest only on restorative strategies, the mathematical program simply decides to relocate the supplying nodes to a less vulnerable location with higher accessibility to gas stations.

By siting a reservoir tank, the new fuel distribution assignment escalates the average fuel mile traveled by 70-150%. The higher distribution cost, however is already paid off by a significant drop in unfilled rate which is the main priority of the model. Adding an extra supplier could also be considered as a compensation strategy for inoperable supply nodes and inoperable arcs, but it cannot maintain the operability of gas stations that are not functional in time of disasters. Therefore, vulnerable gas stations, which include 52% of demand nodes, remain out of the service, if the budget is granted to restorative strategies, exclusively.

In contrary to the first four experiments, experiment 5 encapsulates the sub-properties of the resilience developed in section 2.3.3 and investigates the FSC's operability when the RES are available, simultaneously. Results driven by this experiment are shown in Table 7 and Figure 12.

Table 7. Metrics of experiments

Scenario Number	Available Budget ($M)	RES Cost ($M)	Average mile Flowed by Fuels	UDR	Fuel Supplied by Terminals	Ratio of Supplied Fuel by Terminals (XST/XTD)	Ratio of Supplied Fuel by Tank (XRES/XTD)	Ratio of Budget Spent on		
								Absorptive Strategies	Adaptive Strategies	Restorative Strategies
1	0	N/A	9.427	0.042	129,706	1	0	N/A	N/A	N/A
2	0.5	0	9.427	0.042	129,706	1	0	1	0	0
3	1	0.81	9.427	0.042	129,706	1	0	1	0	0
4	2	1.992	9.933	0.04	132,990	1	0	1	0	0
5	3	2.389	10.31	0.039	136,507	1	0	0.991	0.008	0
6	4	3.936	10.29	0.039	136,510	1	0	0.993	0.006	0
7	5	4.989	10.16	0.039	136,510	1	0	0.99	0.01	0
8	6.5	6.499	17.79	0.008	133,108	0.293	0.706	0.211	0.019	0.769
9	7	6.9595	17.26	0.008	128,595	0.286	0.713	0.267	0.017	0.714
10	8	7.4455	15.03	0.007	126,098	0.279	0.720	0.356	0.018	0.625
11	9	8.6885	19.10	0.006	126,100	0.274	0.725	0.425	0.019	0.555
12	10	9.9645	15.11	0.006	126,100	0.267	0.732	0.477	0.022	0.5
13	11	10.904	21.70	0.005	126,100	0.261	0.738	0.522	0.022	0.454
14	12.5	12.455	16.50	0.004	126,100	0.256	0.743	0.578	0.022	0.4
15	15	14.997	20.92	0.003	128,595	0.251	0.748	0.643	0.023	0.333

16	17.5	17.495	15.69	0.002	126,100	0.230	0.769	0.692	0.021	0.285
17	18	18	26.67	0.002	126,100	0.224	0.775	0.702	0.019	0.277
18	19	18.95	21.35	0.001	129,706	0.226	0.773	0.717	0.019	0.263
19	20	19.996	18.97	0.00084	131,997	0.228	0.771	0.73	0.02	0.25
20	21	20.96	17.61	0.00046	126,100	0.212	0.787	0.742	0.019	0.238
21	22	21.977	16.33	0.00012	126,100	0.209	0.790	0.753	0.019	0.227
22	23	22.755	13.37	0	124,989	0.206	0.7932	0.764	0.018	0.217

Experiment 5

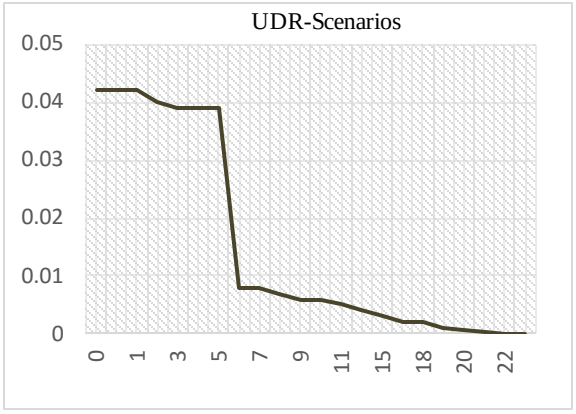

Figure 12.a

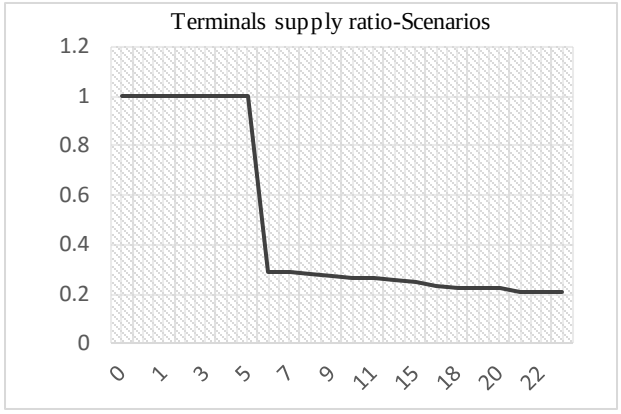

Figure 12.b

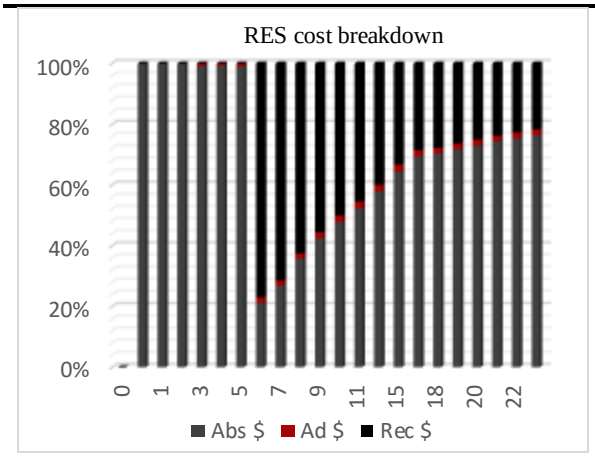

Figure 12.c

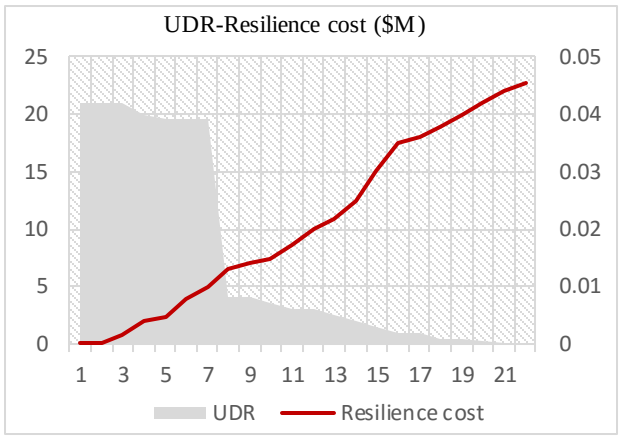

Figure 12.d

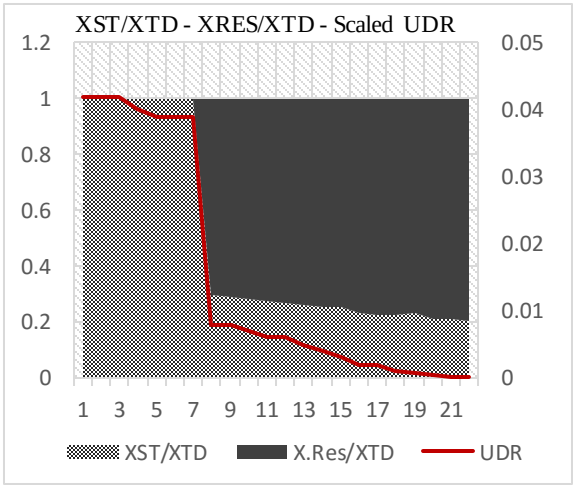

Figure 12.e

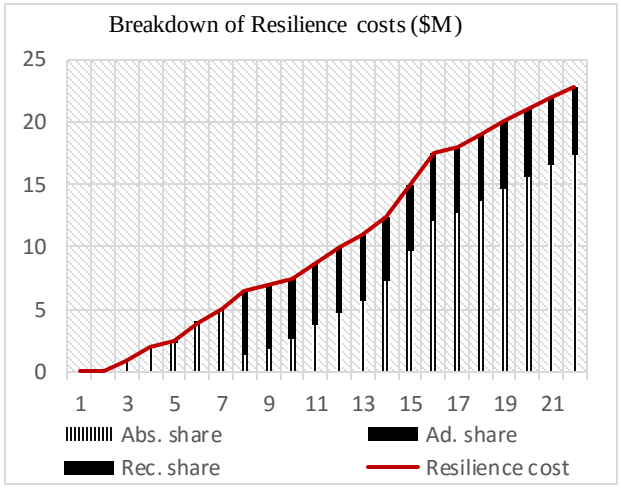

Figure 12.f

Figure 12. Experiment 5 results

Figure 12 illustrates how the FSC's resilience and the average fuel mile traveled ($\bar{X}$/mile) vary in comparison to the results driven by experiments 2-4. As shown in figure 12.a, the triple-RES, together, are capable to drag the UDR down to zero and make the FSC fully operable using a budget of about $20 million.

The breakdown of the RES's cost and its correlation with UDR, as is shown in Figures 12.c and 12.f, is informative. We analyze this in three budgeting frames:

i. Resilience budget under $3 million (scenarios 2-4). The model is not allowed to simultaneously invest in adaptive and restorative strategies, since their costs exceed $3 million. Hence, the model recommends investment on absorptive strategies on transportation network's arcs and by maintaining the network connectedness, decreases the fuel distribution cost by 10 percent.

ii. Resilience budget under $3-$5 million (scenarios 5-7). Here, the model starts investing on the absorptive and adaptive strategies, simultaneously. Though the share of adaptive strategies' cost is about 1%, the FSC's overall resilience improves by 0.3 percent down to 3.9 percent.

iii. Resilience budget above $5 million (scenarios 8-22). Through such case, the model suggests investment actions on all type of strategies. Within any of the budgeting scenarios, the model solution recommends: i) enhancing the robustness of arcs and gas stations, and ii) maintaining the operability of four terminals in Brooklyn and Bronx, where the surge inundation map shows less vulnerability compare to the New Jersey.

In addition, the model solution suggests investments on restorative strategies in which a reservoir tank makes the FSC capable to tackle the supply-deficit caused by inoperable terminals. Similar to experiment 4, the model solution locates the reservoir tank (within the first stage decision) in the location which is optimum against second stage decisions. Through different budgeting restrictions, however, the optimum location of the reservoir tank changes from point to point. This could be a source of complication, if the modeler is planning a time-framed, sequential investment plan. In such a situation, the optimum decisions in time θ, may

hamper the FSC's optimality in time $\theta + n$, when an extra budget is available for further investment.

While the model solution recommends a reservoir tank, by increasing the resilience budget the model limits the number of tank to one and concentrates on absorptive strategies, since the capacity of the implemented tank exceeds Manhattan's daily fuel demand.

As shown in figure 12.d, under the budgeting scenario of $23 million, the FSC becomes fully operable, where the investment shares on absorptive, adaptive, and restorative strategies are about 76, 2, and 22 percentages, respectively. Drawing a comparison between figures 12.c, 12.f, and 12.i on one side and figure 12.d on the other side, it is shown that separate investing on each of the resilience sub-properties (absorption, adaption, and restoration), no matter how large the budget is, cannot improve the system's resilience as much as an investment on a combination of resilience strategies does.

2.6. Conclusion and future work

Resilience, as an infrastructure property, reflects a set of highly correlated characteristics of networks; capabilities to withstand, adapt to, and efficiently recover from the effects of disruptive events. Enhancing the resilience of an infrastructure, however is a process of complementary activities that takes place before (prepositioning of resources to protect the network capacities), during (coping with the imposed inoperability without calling extra resources) and after disruption (recovering from the events' aftermath). To expand our understanding of the concept of resilience and to explore its application in metropolitan critical infrastructures, this paper models Manhattan's motor fuel supply-chain and studied a range of investment portfolios to achieve the optimum network resilience.

The proposed model is developed in two key-steps. The first step is mainly focused on understanding the case study area and data collection; i) drawing the motor fuel supply-chain network that serves the Borough of Manhattan through a Visual Basic-coded application programming interface (VB-API), ii) studying the extreme weather episodes potentially threatening the case study area and investigating their corresponding aftermaths on FSC's elements, and iii) developing a set of candidate strategies enhancing the FSC

robustness in the face of extreme events. Through the second step, we developed a mathematical program to seek the optimum set of RES. The proposed optimization model is developed through a bi-stage integer nonlinear stochastic form. The variables are split into two stages; asset allocation tasks which are the first stage variables, and fuel distribution assignment as the second stage variables. The second stage variables are conditioned on the first stage decisions, where resources are allocated to result the optimum set of second stage decisions.

A series of computational experiments ran to investigate the network functionality given various budgeting restrictions and technical scenarios. The results illustrate how three pillars of RES are interlinked and how different combinations of investment scenarios may provide different levels of resilience. While the proposed model is developed for the Manhattan's motor fuel supply-chain, it provides policy-makers with a fundamental planning tool to address the resilience aspects of the coastal metropolitan's infrastructures which are vulnerable to climate change-induced hazards such as tropical cyclone and sea-level-rise.

The model is fed by the latest input data mainly released by New York State and the NYC, yet these numbers through time can be updated. One of the main obstacles to reliance on such models is data availability, where suppliers, distributers, and retailers are all owned and managed by the private actors who are highly concerned about releasing data. Furthermore, within the past decade, especially following the super-storm Sandy, there have been a number of resilience-enhancing activities taken place in NYC, either through public funds or private sectors investments. Having updates on such improvements would make the model more accurate and save the investors redundant resilience-enhancing actions.

The other key-parameter to take into consideration is legislative flexibilities that federal agencies, State, and City may possibly show in time of disaster, as they did following the super-storm Sandy, to ease or possibly wave some of the fuel transportation restrictions. These restrictions range from the Jones Act (i.e. no foreign-flag tankers can supply fuel from refineries along the Gulf of Mexico) to Environmental Protection Agency - EPA requirements (e.g. local formulation or federal sulfur requirements). Considering such flexibilities in policy implementation provides the City's infrastructures with a higher level of

resilience. Therefore, waiving of restriction policies should be considered as a resilience-enhancing strategy in more case-specific research tasks. The last improving line to suggest is about the socio-behavioral study of the end users. In this research, we simplified the model by assuming that the travelers' post-event behaviors are rational and homoscedastic. While this is a naïve assumption, as shown post super-storm Sandy, the relaxation of this assumption can improve the model significantly.

REFERENCES

1. Aerts, Jeroen CJH, et al. "Cost estimates for flood resilience and protection strategies in New York City." Annals of the New York Academy of Sciences 1294.1 (2013): 1-104
2. Blake, Eric S., Chris Landsea, and Ethan J. Gibney. The deadliest, costliest, and most intense United States tropical cyclones from 1851 to 2006 (and other frequently requested hurricane facts). NOAA/National Weather Service, National Centers for Environmental Prediction, National Hurricane Center, 2007
3. Bruneau M, Chang SE, Eguchi RT, Lee GC, O'Rourke TD, Reinhorn AM, Winterfeldt D (2003) A framework to quantitatively assess and enhance the seismic resilience of communities. Earthquake spectra 19(4):733-752
4. Chen L, Miller-Hooks E (2012) Resilience: an indicator of recovery capability in intermodal freight transport. Transportation Science 46(1):109-123
5. Energy Information Administration (2012) New York City Metropolitan Area retail motor gasoline supply report. https://www.eia.gov/special/disruptions/hurricane/sandy/gasoline_updates.cfm. Accessed 4 December 2015
6. Holling CS (1973) Resilience and stability of ecological systems. Annual review of ecology and systematics 1-23
7. Jenelius E, Mattsson LG (2012) Road network vulnerability analysis of area-covering disruptions: A grid-based approach with case study. Transportation research part A: policy and practice 46(5):746-760
8. Jessup E, McCormack E, Andreoli D, Rose S, Ta, C, Pitera K, Ivanov B (2009) Development and analysis of a GIS-based statewide freight data flow network (No. WA-RD 730.1). Washington State Department of Transportation

9. Koch, James V. "Costs of defending against rising sea levels and flooding in Mid-Atlantic metropolitan coastal areas: The basic issues." Journal of Regional Analysis & Policy 40.1 (2010): 53
10. Lee HL (2004) The triple-A supply-chain. Harvard business review 82(10):102-113
11. Lou Y, Zhang L (2011) Defending transportation networks against random and targeted attacks. Transportation Research Record: Journal of the Transportation Research Board (2234):31-40
12. Miller-Hooks E, Zhang X, Faturechi R (2012) Measuring and maximizing resilience of freight transportation networks. Computers & Operations Research 39(7):1633-1643
13. Murray-Tuite P, Mahmassani H (2004) Methodology for determining vulnerable links in a transportation network. Transportation Research Record: Journal of the Transportation Research Board (1882):88-96
14. National Association of Convenience Stores (2013) How hurricane Sandy affected the fuels industry. http://www.nacsonline.com/YourBusiness/FuelsReports/GasPrices_2013/Pages/How-Hurricane-Sandy-Affected-the-Fuels-Industry.aspx. Accessed 4 December 2015
15. NYC (2013) A Stronger, More Resilient New York. http://www.nyc.gov/html/sirr/html/report/report.shtml. Accessed 4 December 2015
16. Omer M, Mostashari A, Nilchiani R (2011) Measuring the resiliency of the Manhattan points of entry in the face of severe disruption. American Journal of Engineering and Applied Sciences 4(1): 153-161
17. Ponomarov SY, Holcomb MC (2009) Understanding the concept of supply-chain resilience. The International Journal of Logistics Management 20(1):124-143
18. Rawls CG, Turnquist MA (2010) Pre-positioning of emergency supplies for disaster response. Transportation research part B: Methodological 44(4):521-534
19. Rawls CG, Turnquist MA (2011) Pre-positioning planning for emergency response with service quality constraints. OR spectrum 33(3):481-498

20. Rawls CG, Turnquist MA (2012) Pre-positioning and dynamic delivery planning for short-term response following a natural disaster. Socio-Economic Planning Sciences 46(1):46-54
21. Responding to Climate Change in New York State: The ClimAID Integrated Assessment for Effective Climate Change Adaptation in New York State: Final Report. Blackwell Pub., 2011
22. Soni, U, Jain, V (2011, December) Minimizing the vulnerabilities of supply-chain: a new framework for enhancing the resilience. In Industrial Engineering and Engineering Management (IEEM), 2011 IEEE International Conference on (pp. 933-939). IEEE
23. Sullivan JL, Novak DC, Aultman-Hall L, Scott DM (2010) Identifying critical road segments and measuring system-wide robustness in transportation networks with isolating links: A link-based capacity-reduction approach. Transportation Research Part A: Policy and Practice 44(5):323-336
24. Tang CS (2006) Robust strategies for mitigating supply-chain disruptions. International Journal of Logistics: Research and Applications 9(1):33-45
25. Tsvetanov, Tsvetan G., and Farhed A. Shah. "The economic value of delaying adaptation to sea-level rise: An application to coastal properties in Connecticut." Climatic change 121.2 (2013): 177-193
26. Tsvetanov, Tsvetan G., and Farhed A. Shah. The Economics of Protection against Sea-Level Rise: An Application to Coastal Properties in Connecticut. No. 10. 2012
27. Tomlin B (2006) On the value of mitigation and contingency strategies for managing supply-chain disruption risks. Management Science 52(5):639-657
28. Turnquist MA, Vugrin E (2013) Design for resilience in infrastructure distribution networks. Environment Systems & Decisions 33(1):104-120
29. Vugrin ED, Turnquist MA, Brown NJ (2014) Optimal recovery sequencing for enhanced resilience and service restoration in transportation networks. International Journal of Critical Infrastructures 10(3-4):218-246g

CHAPTER 3

FLOOD-RESILIENT DEPLOYMENT OF FUELING STATIONSS: AN EXTENSION TO FACILITY LOCATION PROBLEM

3.1. Introduction

In the past few years, extreme weather episodes have exposed the lack of resilience across critical metropolitan infrastructures and revealed how the vulnerability of physical networks hampers overall functionality of urban America. In response to the increasing number of extreme events, a number of research domains, such as 'disaster preparedness planning' and 'resilience planning', have stepped into the modeling area and developed a range of quantitative/methodological approaches to model under-attack critical infrastructures such as power grids, natural gas pipelines, and more recently transportation networks.

However, a majority of the models and analytical approaches investigated the resiliency of transportation network, either solely or in association with interdependent infrastructures such as transit and power grid. Given the existence of such interdependencies, considering these infrastructures separate from each other is neither sufficient nor exhaustive. Transportation networks are, however, interdependent with many other urban systems such as the motor fuel supply-chain. The interconnectedness between the transportation network and motor fuel supply-chain (FSC), inevitably, makes the functionality of the FSC as critical as the transportation network's operability. More specifically, the FSCs' inoperability has direct impact on transportation networks, as well as indirect influence on other infrastructures performing interdependently with transportation networks.

For instance, following the Superstorm Sandy, the FSC of New York City (NYC) faced extensive inoperability; failure rippled along interdependent critical infrastructures (ICI) such as transportation and transit networks. Direct and cascading failures on the City's transport system interrupted the daily life of millions of New Yorkers and imposed billions of dollars of costs on the regional economy. The storm and its aftermath highlighted how failure of the fueling supply-chain could disrupt a transportation

infrastructure, and how inoperability of a transportation network could disturb the process of fuel distribution.

Despite all the efforts made by the City of New York and energy operators, full restoration took weeks and cost billions of dollars. A set of resilience-enhanced infrastructures along the fueling supply-chain could ease the ICI's adaptation to emerging vulnerabilities and could save the City from the long and costly recovery process. In spite of a number of works focusing on supply-chain resiliency, whether in regional, national, or intercontinental level, urban-scaled motor fuel supply-chain behavior has been less investigated, particularly when the infrastructure is faced with extreme weather events.

Herein, we apply the concept of ICI in the context of disaster preparedness planning and study an optimum set up of a fueling network that is robust in time of disasters. The proposed model makes a bridge between three systems of i) transportation network, ii) motor fuel supply-chain, and iii) the extreme weather episodes potentially threatening metropolitan areas. In fact, the model is an extension of the facility location problem and provides an optimal deployment portfolio for fueling stations, considering transportation network's random operability in the face of extreme events. Through a multi-stage stochastic program, the model expands the fueling stations network, either through prepositioning a new set of service facilities or by enhancing the capacity of current facilities.

The first key contribution of this paper is our novel disaster-modeling framework, which can be adapted for many other hazards-threatening metropolitan areas. Our proposed model provides a new approach to integrate federally-funded hazard assessment models such as Hazus-MH and Flood Insurance Rate Map (FIRM) with graph-based urban infrastructures. The second key -contribution is the new insight to take a tri-layer ICI into consideration for urban-scale disaster preparedness planning. In short, the proposed model is aimed to provide transportation networks with resilient and less vulnerable sources of motor fuel, and this should be considered as a significant improvement on ICI operability, particularly when stressed or under attack.

3.2. Literature Review

Within the pool of supply-chain and risk management articles, resilience is defined as a property which encapsulates several network's characteristics. Lee (*1*) presented a 'triple-A' aspects of resilient supply-chain as agility, adaptability, and alignment. Bruneau et al. (*2*), however elaborated four 'complementary measures' of robustness, redundancy, resourcefulness, and rapidity in recovery. Ponomarov and Holcomb (*3*) also discussed over three steps of readiness, response, and recovery and Soni and Jain (*4*) introduced flexibility, visibility, collaboration, adaptability, and sustainability as required attributes to support the supply-chain resilience. Lastly, Turnquist and Vugrin (*5*) discussed over the concept of resiliency in supply-chain domain and explored 'resilience-enhancing investments' through aspects of absorption, adaptation, and restoration.

Despite the 'divergent definitions' and 'conceptual vagueness' of the term resilience (*6*)-(*8*) there are a few common dots within a majority of the research domains; i) resilience, as a system property, represents the capability of infrastructures to experience minimum inoperability in time of disaster, ii) resilience enhancing strategies (RES) are framed within three time windows of pre, during and post shock, and iii) a resilience-enhancing plan is an aggregated set of absorption, adoption, and restoration activities which leads infrastructures into the pre-disturbance state.

By relying on existing literatures, we recognize the term resilience as an aspect of the systems to better withstand and absorb, efficiently adapt to, and quickly-cheaply recover from the inoperability imposed by potential extreme events. Besides the illustrative and conceptual articles, few quantitative methods have been developed to address infrastructures resilience. Herein, we summarize these quantitative approaches into three threads.

- A series of research articles considers RES that take place prior to extreme events arrival and make the infrastructures more robust to absorb and cope with such events. This category ranges from resource allocation models to reinforcement modeling of network components.

- In contrast to the models that include pre-event RES, a line of works assesses a series of post-event strategies (i.e. recovery actions) augmenting the resilience capability of infrastructures.
- The third thread of works explores a range of candidate pre- and post-event RES, simultaneously.

Aside the concept of resiliency, we divide the models that are commonly used under the umbrella of facility location problem, into eight categories.

One - Fixed-charge facility location problem is a classic location problem that investigates the subset of candidate locations which minimizes the distribution cost of flow from supply nodes to demand locations. Within the fixed charge problem, two series of decisions must be made i) decisions regarding the location of facilities and ii) distribution task decisions. The first line of decisions includes fixed-charge costs and the second line of decisions imposes trans-shipment costs. This model has been used in a number of fields of studies and through many applications such as supply-chain management (*9-10*) and distribution-center siting (*11-12*).

Two – The Maximal Covering location problem (MCLP), introduced in 1970s (*13*), is developed to serve case studies with insufficient resource/budget. MCLP. Therefore, it takes *P* as the fixed number of facilities and investigates the optimal location of facilities to cover demand as much as possible. Kuby and Lim (*14*) implement the Maximal Covering problem through the concept of 'flow capturing' and demonstrated a 'greedy-adding' approach through sub-optimality. They conceptualized 'flow refueling location problem' (FRLM) base on 'flow capturing facility location models' (FCLM) which was originally developed by Hodgson's (*15*), and further extends the solution methods through development of heuristic algorithms (*16-17*).

Three –Set Covering location problems (SCLP) minimize the location costs satisfying a specified level of coverage. Precisely, by defining a threshold level for distribution cost (costs could be dollar value, distance or time), the SCLP minimizes the number of facilities capable to serve demand and assures no distribution action will cost the objective function more than the predefined threshold level. SCLP has also been extended through flow capturing concept and FCLM (*18-19*).

Four – *p*-median, as an NP-hard problem, locates *p* number of facilities in order to minimize the distribution cost for satisfying demand, while each of the demand points is supplied from the nearest located facilities. Two key-decisions (*20*) for this model are i) where to locate *p* number of facilities and ii) what demand point should be served by which supplier.

Five – Maximum Covering/Shortest Path problem (MCSPP) developed by Current et al. (*21*) as a bi-objective integer program. The first objective is to identify the shortest path between supply and demand nodes; whereas, the second objective is to maximize the total satisfied demand. The MCSPP, technically solves a 'mini-sum' and 'maxi-sum' problems for the first and second objectives, respectively.

Six – Fuel-travel-back model, which is relied on 'flow-capture' technique, locates service facilities in the shortest distance to where drivers consume fuel. Lin et al. (*22*) conceptualized this approach based on assumption that "where you drive more is where you more likely need refueling." To this end, the model locates fueling nodes in the closest distance to demand points, where demand points are transportation networks' arcs. Every single arc provides a particular demand driven by the ratio of total vehicle mile traveled (VMT) to averaged fuel efficiency rate.

Seven – Agent-based modeling (ABM) has been used recently, as an alternative modeling technique to address shortages corresponding to optimization-oriented methods; shortages such as the lack of interaction with social and behavioral systems, high computational complexity that requires modelers to approximate the solution through heuristics (*23*), concurrently distributed domains (*24*), and non-integrated platform with 'Information Systems' like GIS (*25*). The application of ABM in the facility location problems has three elements; i) a set of agents with attributes and behaviors, ii) a set of relationships and methods of interaction, and iii) the agents' environment (*26*). Han et al. (*27*), through a Starlogo simulation platform, discussed the principle of rationality and related factors for the gas station layout and determined the relationship between the number of stations and motor vehicle demand.

Aside the location problem for gas stations, the ABM also is used as a decision support system to identify the allocation of the electrified charging stations (*28*). In (*25*), Han et al. implemented this approach to

assess and determine the strategic locations for public charging stations. They implemented the ABM method align with GIS to illustrate the spatial distribution of service stations in 2020 and provided different stakeholders with a decision support tool to gather information about locations and quantities of charging points.

Eight – Hybrid models, which include the advantages of ABMs and pure optimization, are developed under two approaches; i) applying an optimization technique to the problem, then re-plan the solution by agents and ii) embedding optimization rules in agents and the simulation (*29*).

This article advances the concept of location problem within the context of resiliency. To this end, we develop a new methodology which reflects the importance of ICIs' operability in time of disaster.

3.3. Methodology

Much effort is invested to develop theoretical approaches through modeling the behavior of interconnected infrastructures and the resiliency-enhancing strategies towards sustainable ICIs. Yet, cities' concerns have not been limited to feasibility studies or technical reports, and in recent years shifted to financial investments and physical developments across vulnerable and critical infrastructures. In view of this, there are key-factors in resilience-enhancing models which have not been fully addressed in technical reports or in the recent developments. Notably, the interdependency across transportation and motor fuel supply-chain networks has been overlooked, as well as the impact potential extreme events may impose on these infrastructures. To fill this gap in modeling approaches, an integrated set of resilient infrastructures should be designed to i) represent the transportation and FSC networks as an ICI, and ii) optimize the ICIs' resiliency when it is disrupted or under attack. To perform so, we develop a three-step strategy to address criteria discussed above.

To illustrate the methodology, we design an experimental testbed graph, shown in Figure 1, and conceptualize the simplified version of the proposed model on this illustrative graph. The testbed represents a sample platform including 48 land parcels, 19 nodes, and 37 links. Vulnerable areas to extreme events are also predefined and color-coded through lands vulnerable to i) 100-year floods and ii) 500-year floods.

Step one – Modeling network inoperability

Through the first step, we develop a testbed graph, as is depicted in Figure 13 and simulate a subset of extreme events that may threaten the case study area. Noting that among the range of natural hazards, the proposed research concentrates on flooding impacts as a sample case for extreme events. Through a subset of flooding types, two disaster scenarios can be defined: flood hits the case study area with a return-period of 100-year (scenario 1) and 500-year (scenario 2). In addition to these two extreme events, we simply define the third complementary scenario representing the time no disaster or extreme event strikes the ICI. Each of the first two scenarios has its own characteristics including; i) frequency of arrival, ii) type of threat, iii) expected intensity, and iv) corresponding vulnerable locations. If one of these scenarios arrives, the ICI experiences some levels of inoperability due to flooded arcs located in vulnerable zones. The disrupted ICI, consequently, hampers commuters travel behavior. Thereby, commuters may change their route, departure time, travel mode, destinations, or even some of them may cancel their trips. Consequently, we can model a new set of traffic assignments for the first two scenarios. On the other hand, the ICI performs as business as usual (BAU) under the third scenario, when the networks' elements are fully functional, meaning there is no change on traffic assignment in the third scenario. Consequently, there are three *O-D* tables corresponding to triple scenarios. Vulnerable zones related to triple-scenarios are color-coded in Figure 13.

Now, consider the testbed network. There is an *O-D* table calibrated for each scenario, which may include vehicle classes. With respect to traffic assignments, find the network's link volumes. Let v_a^m be the volume for class *m* on link a. Then, project the *VMT* (by vehicle class) on link a to the destination node of that link, node j, and sum the values of node j to represent the *VMT* to reach this node. If all vehicle classes use the same fuel, aggregate *VMTs*, otherwise, keep them separate. Dividing the aggregated *VMT* at node j over the expected fuel efficiency rate, q_j represents amount of fuel burned on immediate prior links to the node j. The output of this step is three sets of node-based fuel consumption rates. Each set corresponds to a scenario that the case study area might be faced with.

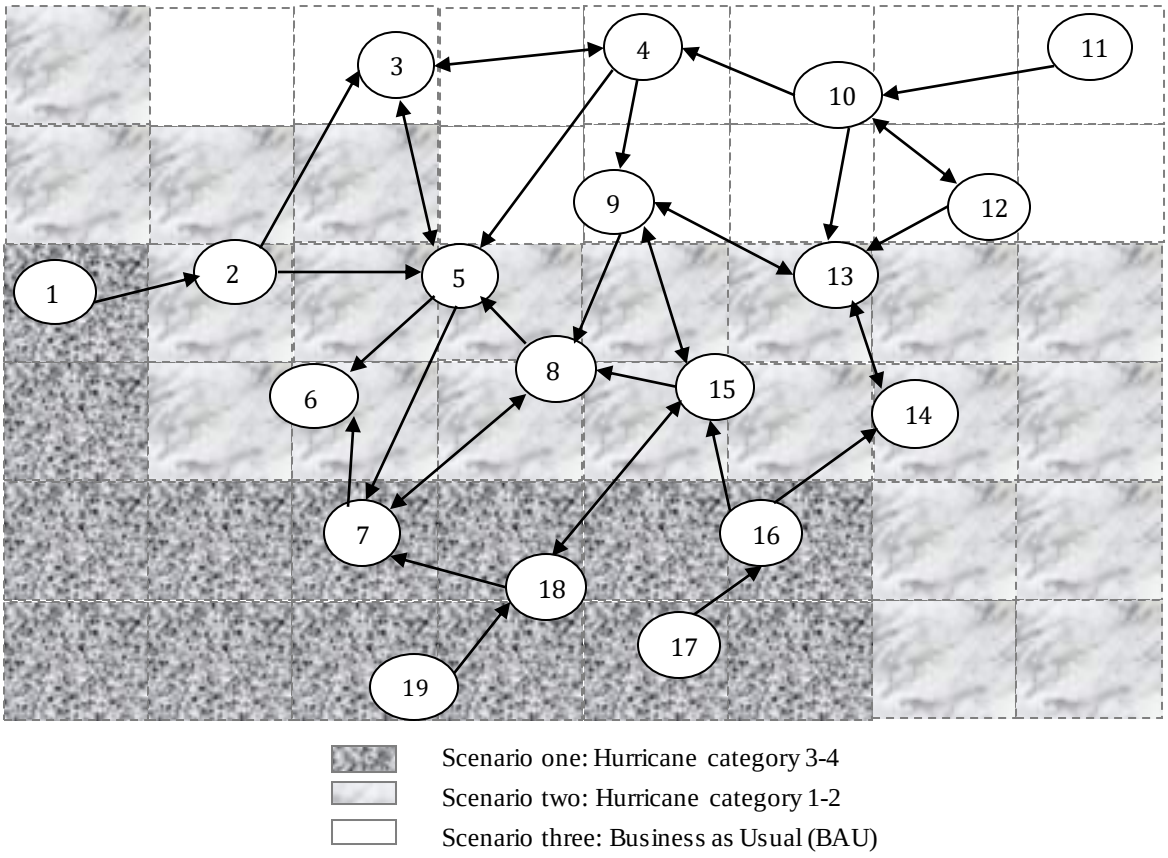

Figure 13. Color-coded vulnerable zones

Step two – Modeling the ICI

This step is aimed at modeling an integrated set of infrastructures reflecting the existing interdependencies among transportation and FSC networks. To model such interdependency, we adopt the model developed by Lin et al. (*22*) and associate the travel behavior of commuters with location, operability state, and capacity of fueling stations located across the FSC. As discussed in section 2 and with respect to the notion of "where you drive more is where you more likely need refueling," we make a bridge between 'where commuters drive' and 'where they need to refuel.'

For now, assuming there is no existing FSC network, we need to locate such an infrastructure across an urban area (later in section 4, we relax this condition and extend the model into real world situation where FSC is existing, but might be vulnerable to extreme weather). Consequently, the modeler's main goal is

designing a FSC (i.e. locating gas stations) with optimum operability. The FSC optimality could be discussed through a number of parameters such as i) shortest path between 'where commuters refuel' and 'where commuters drive,' ii) the minimum expected travel time deviation between refueling-trips and ordinary trips, iii) minimum social cost driven by refueling-trips, or iv) a combination of these parameters. Without loss of generality, assume the cost of serving fuel demand at node *j* by a station at node *i* is distance-based, using d_{ji} for distance from point j to point i. Add to this distance the average distance across links terminating at j (for the flows aggregated at node j). Call this distance l_j. Then define cost as $C_{ij} = (d_{ji}+l_j)\varphi$, where φ is a cost per mile. Decisions to locate or expand the fueling network depend on i) minimizing distance-based cost of meeting fuel demand, ii) ensuring coverage of most of demand (i.e., a fueling location within D miles for at least a percentage of demand), iii) deployment cost of stations, and iv) station capacity available at node i. For now, consider just one fuel class: gasoline (m=1). Define variables and input values as noted in Table 8.

Table 8. Input Parameters and Variables Descriptions

Variables	
y_i	1 if fueling facility is available at node i; 0 otherwise
x_{ij}	Fraction of refueling demand at j assigned to be served at node i
Parameters	
G_i	Available capacity of station(s) at node i
U	System's operability level
Q	Total demand ($\sum_j q_j$)

Then, optimum deployment of fueling stations could be solved through the following bi-stage linear program.

$$\text{Min} \quad \sum_i y_i + \sum_i \sum_j C_{ij}\, x_{ij} q_j \tag{3.1}$$

s.t. $\sum_i x_{ij}=1$ $\forall$ j (3.2)

$\sum_j x_{ij} q_j - G_i y_i \leq 0$ $\forall$ i (3.3)

$\sum_i \sum_j x_{ij} q_i \geq UQ$ $\forall$ i,j (3.4)

$x_{ij} \geq 0$ $\forall$ i, j (3.5)

$y_i \in \{0, 1\}$ $\forall$ i (3.6)

Objective function (3.1) deploys a minimum number of gas station required to meet the system's operability index, given the least fuel distribution cost. The objective consists of two stages of variables. The first-stage locates fueling stations, while the second-stage seeks the minimum cost to meet the system's operability index. The former stage, however, is conditioned on the latter one, and the model finds solutions for both stages, simultaneously. Constraint (3.2) forces all demand to be assigned somewhere. Constraints (3.3) and (3.4) represent flow conservations and constraints (3.5) and (3.6) reflect variables' feasibility.

Step three – Modeling a set of resilient ICI

By integrating the first two steps, step three investigates the optimal deployment task given i) distribution of fuel demand across the transportation network and ii) scenarios that a given ICI may face with.

The randomness across events' arrival casts the problem discussed in step two into a form lending itself well to a bi-stage stochastic problem. Herein, the objective function is split into three portions, each corresponds to a scenario. Each portion comes with a particular network specification based on a network's operability state related to the corresponding scenario. Though each of the scenarios, individually, may have a different optimal solution, the weighted average objective function might be optimal through a set of first-stage decisions that have not been chosen for any individual scenario. Given this fact, the stochastic bi-stage program, seeks a deployment task of fueling stations which optimal against the minimum fuel

distribution cost in the face of flooding scenarios. If set $s = \{1, 2, 3\}$ defines scenarios and p_s represents probability of scenario s, the objective function (3.1) extends to the following form:

$$Min \qquad \sum_i y_i + \sum_s p_s \sum_i \sum_j C_{ij}^s x_{ij}^s q_j^s \qquad (3.7)$$

Within the objective function (3.7), the second-stage variable is weighted over the scenarios occurrence chance. Precisely, the deployment task locates gas stations in such a way to maximize the random functionality of transportation network over the course of triple-scenarios.

3.4. Illustrative Case Study

The methodology introduced in the previous section has been applied to investigate the optimum fuel deployment in center business district (CBD) of the city of Fresno, CA. The case study covers an area of 27 sq. mile, including 34 gas stations operating under different brands. According to the Federal Emergency Management Agency (FEMA), the city of Fresno is vulnerable to two categories of flooding event: i) 1% annual chance flood hazard (ACF) and ii) 0.2% ACF. Therefore, the case study area may experience two types of extreme event. We, as modelers, can simply simulate the aftermath of these events by defining two distinct scenarios and investigating the ICI's operability given the functionality of networks' elements under each scenario. Simulating the ICI's operability in the face of each of these scenarios is straight forward. Functionality of the ICI's element is relaxed (the element becomes inoperable), if i) the element is located within the hazard zone corresponding a given scenario and ii) the hazard associated to the scenario is arrived. In addition to these two scenarios, the third scenario represents the ICI's functionality while the city of Fresno is struck by no extreme event (i.e. the ICI functions as BAU).

To show the transportation network and existing location of service stations, online search[25] has been performed and results exported to an ArcGIS layer, as shown in Figure 14. This Figure represents location

[25] fresnogasprices.com

of existing gas stations and vulnerability zones associated with each scenario. During the first scenario, when a flood with a 100-year return-period strikes, FSC and transportation networks experience partial inoperability. Across the FSC, five gas stations are located in vulnerable zones and are inoperable during this scenario. Likewise the FSC, transportation network would be partially inoperable due to flooded links and surge inundation level in vulnerable zones.

As shown in Figure 14, during a 100-year flooding scenario, the case study area will be separated into two distinct parts due to the existing flood canal stretching from the far West to the North-east of the case study area. On the other side, if a 500-year flood arrives (i.e. scenario two), the ICI performs differently; more than 70% of gas stations (i.e. 24 gas stations) and about half of the transportation network's elements located within the corresponding vulnerable zones go out of the service. Contrary to disruption scenarios, during the BAU scenario, both FSC and transportation networks are fully functional. Due to inoperability of vulnerable links in time of disasters, traffic analysis zones (TAZs) within the color-coded vulnerable areas cannot generate or attract trips. Whereas, TAZs located in no-flooding areas remain functional. However, the latter type of TAZs can only generate or attract trips passing through invulnerable areas.

In other words, travel demands that cannot find paths through their destination within unflooded links remain unmet. In fact, a given travel demand is met if i) corresponding origin and destination are located in unflooded zones and ii) there is at least one path to pair up origin and destination. In time of disaster, transportation network experiences some degrees of disruption, whether through unmet demands or higher rate of VMT imposed by supply deficit. Yet, such dysfunctionalities could be tackled through a new set-up for FSC network. Such set-up enhances the fueling network's robustness through locating new gas stations, expanding the capacity of current facilities, or both.

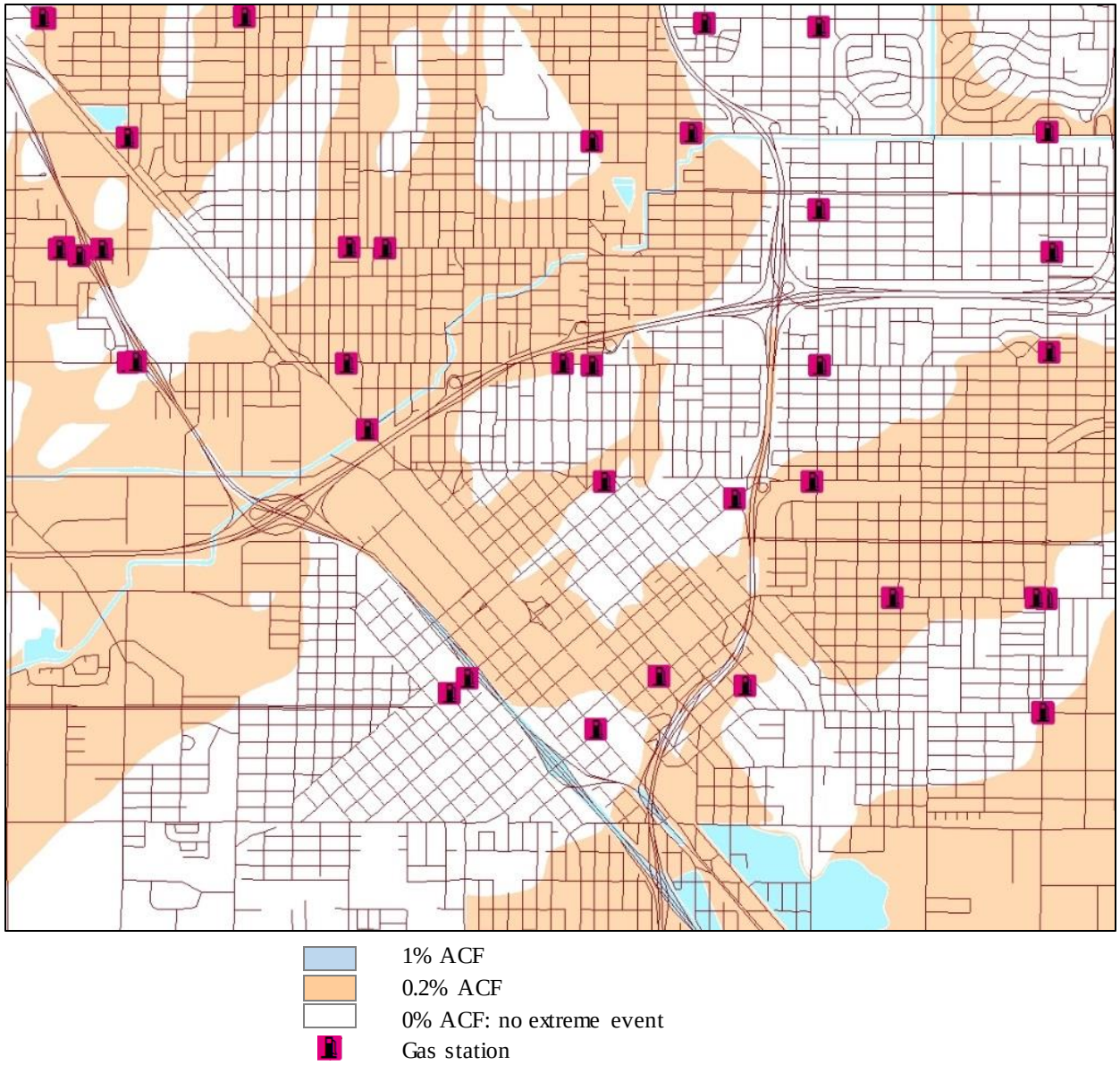

Figure 14. Existing gas stations across the case study area and FEMA flood hazard areas

Table 9. Nomenclature

Sets	
$\{s\} = \{1, 2, ..., S\}$	Scenarios
$\{i\} = \{1, 2, ..., I\}$	Gas stations
$\{j\} = \{1, 2, ..., J\}$	Demand nodes
$\{c\} = \{1, 2, ..., C\}$	Capacity levels

$\{\beta\} = \{1, \ldots, B\}$	Capacity-enhancing strategies

Parameters	
$\mathbb{L}$	A large number
$\mathbb{P}_s$	Occurrence chance of scenario s
C_{ij}	Delivery cost of a gallon of fuel from gas station in node i to demand node j
$D_{i,\beta,c}$	Dollar value of implementing strategy β with capacity c in node i
G_i^s	Existing capacity of gas station in node i during scenario s
$G'_{\beta,c}$	Corresponding capacity to strategy β with capacity c
q_j^s	Demand at node j during scenario s
Z^s	1 if scenario s is included in reliability set for coverage; 0 if not
Q^s	Total demand during scenario s
U^s	Fraction of demand that must be met during scenario s
$\boldsymbol{\alpha}$	Required reliability level ($0 \leq \boldsymbol{\alpha} \leq 1$)
d_{ij}^s	Shortest path between gas station i to demand node j over the network operable in scenario s
d_a	Length of arc a
l_j	Average distance across links terminating at node j (for the flows aggregated at node j)
V_a^s	Vehicle volume on link a in scenario s
FER	Fuel efficiency rate

Decision variables	
X_{ij}^s	Transshipped flow from gas station i to demand node j
$Y_{i,\beta,c}$	Binary variable; 1 if strategy β with capacity c is chosen for node i, 0 if not

Based on input parameters and model variables described in Table 9, the optimization model is formulated as the following bi-stage stochastic linear program.

$$Min \quad \mathbb{L} \cdot \sum_s \mathbb{P}_s \sum_i \sum_j C_{ij}^s X_{ij}^s + \sum_i \sum_c \sum_\beta Y_{i,\beta,c} D_{i,\beta,c} \quad (8)$$

$$s.t. \quad \sum_j X_{ij}^s \leq G_i^s + \sum_\beta \sum_c Y_{i,\beta,c} G'_{i,\beta,c} \quad \forall\, i, s \quad (9)$$

$$q_j^s \geq \sum_i X_{ij}^s \quad \forall\, j, s \quad (10)$$

$$\sum_i \sum_j X_{ij}^s + (1\text{-}Z^s) Q^s \geq U^s Q^s \quad \forall\, s \quad (11)$$

$$\sum_s \mathbb{P}_s Z^s \geq \boldsymbol{\alpha} \quad \forall\, s \quad (12)$$

$$\sum_\beta \sum_c Y_{i,\beta,c} \leq 1 \quad \forall\, i \quad (13)$$

$$Q^s = \sum_j q_j^s \quad \forall\, s \quad (14)$$

$$C_{ij}^s = d_{ij}^s + l_j \quad \forall\, i, j, s \quad (15)$$

$$q_j^s = [\sum_{a \to j} (d_a . V_a^s)] / FER \quad \forall\, j, s \quad (16)$$

$$X_{ij}^s \geq 0 \quad \forall\, i, j, s \quad (17)$$

$$Y_{i,\beta,c} \in \{0, 1\} \quad (18)$$

$$Z_s \in \{0, 1\} \quad (19)$$

The objective function (3.8) elaborates both stages of variables: facility deployment and flow distribution. The former stage, as an asset allocation model, assigns capacity-enhancing strategies across the FSC in order to reach the second-stage's optimum value. The latter stage variables, X_{ij}^s, in turn, investigate the optimum fuel distribution pattern including i) location of supply and demand nodes, ii) quantity of flows assigned for each supply and demand nodes, and iii) shortest paths corresponding to distribution pattern. The second-stage variables are technically conditioned on the first-stage decisions, and the model seeks to find the set of first-stage variables that are optimal against the outcomes driven by the second-stage. The outcome of the second-stage decisions, however, is randomized through the scenarios' associated probabilities, $\mathbb{P}_s$.

While the first part of the objective function investigates the flow assignment, the second part protects resources for being invested inefficiently. The constant $\mathbb{L}$ is included in the first part of the objective, as a coefficient ($\mathbb{L} >> \sum_i \sum_c \sum_\beta Y_{i,\beta,c} D_{i,\beta,c}$), to assure the priority of optimal distribution pattern over the investing strategies. Constraint (3.9) is a flow conservation constraint at node *i*, and assures the distribution solution does not exceed available fuel at node *i*.

Available fuel at node *i* could be supplied through either the non-disrupted and existing fuel capacity at node *i*, enhanced-capacity through the proposed investment, or both. Constraint (3.10) limits incoming flow to demand node *j* below the corresponding demand volume. Constraint (3.11) is the coverage requirement, which operates in conjunction with constraint (3.12) to assure that the probability is at least $\boldsymbol{\alpha}$ that a fraction U^s of total demand is covered in scenario *s*. The U^s requirement for a 'mild' scenario (a 100-year flood) may be higher than in more severe ones, for example. Constraint (3.13) stops the model from investing on more than one strategy at node *i*. Constraints (3.14) -(3.16) define input parameters and constraints (3.17) -(3.19) assure the non-negativity and feasibility of variables, respectively.

3.5. Computational Experiments

To run the transportation model, we used the Fresno travel demand model version (2003), and we run the model to estimate the 2030 traffic flow pattern. To explore various aspects of the model, ten numerical experiments have been implemented. To do so, a range of input parameters has been defined for two constants of Z^s and U^s. Input parameters corresponding to experiments are shown in Table 10.

Table 10. Input Parameters

Experiment number	$\mathbf{Z^s}$			$\mathbf{U^s}$		
	$\mathbf{Z^1}$	$\mathbf{Z^2}$	$\mathbf{Z^3}$	$\mathbf{U^1}$	$\mathbf{U^2}$	$\mathbf{U^3}$
1	1	0	1	0.75	-	1
2	1	0	1	0.9	-	1
3	1	0	1	1	-	1

4	1	1	1	0.75	0.5	1
5	1	1	1	0.75	0.75	1
6	1	1	1	0.9	0.5	1
7	1	1	1	0.9	0.75	1
8	1	1	1	1	0.5	1
9	1	1	1	1	0.75	1
10	1	1	1	1	1	1

All experiments are based on combinations of minimum demand ratio that must be met in a scenario (U^s) and included scenario(s) in reliability set for coverage (Z^s). Through the experiments, two series of enhancing strategies, six strategies in total, have been explored:

- enhancing the supply capacity of the existing gas station by 20%, 30%, and 40% (strategies **a**, **b**, and **c**, respectively)
- deploying a new gas station with 80%, 100%, and 125% of the averaged supply capacity of the existing gas stations (strategies **d**, **e**, and **f**, respectively)

Figure 15 summarizes the experiments' results, and Figure 16 shows how the proposed model, with respect to imposed reliability-coverage restrictions, would enhance/deploy a range of service facilities across the FSC. As shown in Figure 15, by increasing the intensity of flooding episodes and increasing the reliability level of the FSC, the required budget to maintain the system's reliability level escalates. However, the corresponding curve to the minimum required budget shows different slopes through the range of experiments. For instance, experiments 6 and 10 experience mild slope compared to other experiments. The main reason for such one pattern is slight changes on FSC requirements, in both experiments, with respect to requirements needed for the immediate prior experiments (namely, experiments 5 and 9).

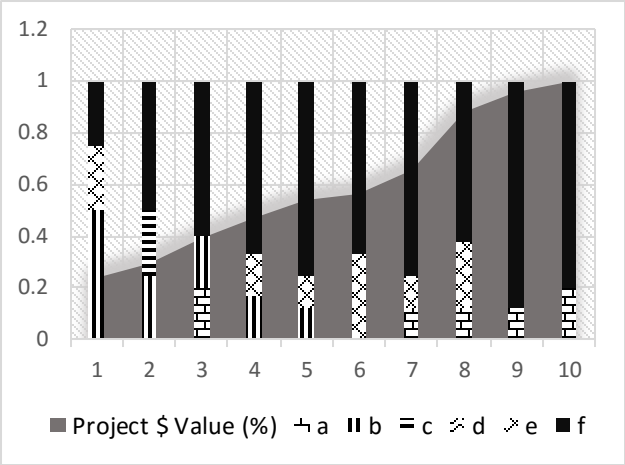

Figure 15. Experiments Results

Moreover, by increasing the system requirements/reliability level, the model invests on more new constructions with larger capacities; whereas, in early experiments, objective function's choices are mainly focused on enhancing capacities of existing facilities.

The location of deployed/enhanced facilities, as shown in Figure 16, changes over the experiments. The FSC faces no restriction to deploy facilities in experiments 1 to 3. Precisely, in these three experiments, facilities can be deployed across the network with no limitations. This happens due to the geographic dispersion of vulnerable zones corresponding to a 100-years flood. As discussed in section 4, corresponding vulnerable zones to scenario 1 are only stretched over the flood canal, and the rest of the case study area can host new facilities. Consequently, a number of investments are put in areas that are recognized as the scenario-two's vulnerable zones. On the other side, deployed facilities in the last experiments (experiments include both scenarios 1 and 2) are entirely located on safe zones with no chance of flooding.

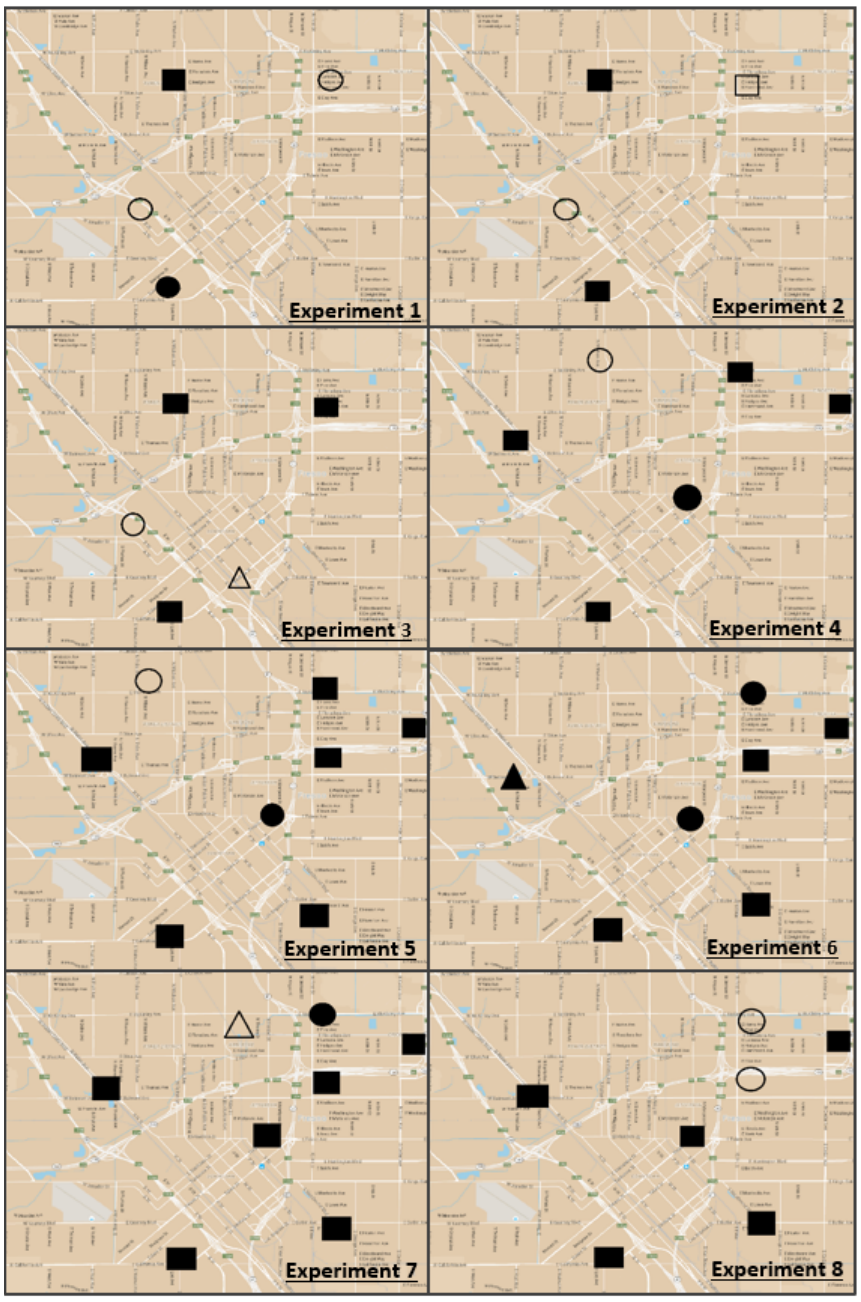

Strategy	Icon	
		Deployment of new facility
a	▲	20%
b	●	30%
c	■	40%
		Enhancing existing capacity
d	△	80%
e	○	100%
f	□	125%

Figure 16. Distribution of assets corresponding to capacity-enhancing strategies in experiments 1-8

3.6. Conclusion

The concepts of system of systems (SOSs) and interdependencies across metropolitan critical infrastructures have been around for decades, although relevant analytical methodologies and empirical studies have been less developed. This research gap can be justified by a number of key reasons, namely: complexity of topic, scale of problems, difficulties of gathering data and information from separate firms, lack of adequate computational tools/skills, and etc.

However, recent pioneering improvements in data management and advancing of analytical tools provide better foundation for in-depth studies of ICIs' behaviors. In addition to an emerging understanding of infrastructures' interdependency mechanism, reliability of metropolitan key-infrastructures and the importance of their operability are also becoming increasingly important as indicators of national security and economy stability. However, recent focuses on reliability of ICIs are mostly on either vulnerability analysis or infrastructure recovery plans. Though investigation of both topics are necessary steps towards determining ICIs' sustainable design, a more comprehensive approach is needed to develop a set of integrated strategies assisting infrastructures to better cope with extreme events.

In this article, we studied the operability of motor fuel supply chain in downtown Fresno, CA. To do so, fuel infrastructure's functionality examined through three scenarios which reflect real world occasions: (1) business as usual, (2) a 100-year flood, and (3) a 500-years flood. The results shows how investment on resilience-enhancing strategies can provide the ICI with a higher level of robustness and how assets and resources could be allocated across the network's elements, optimally and efficiently.

Although analytical methods for modeling the infrastructures' interdependency and resiliency of this ICI during extreme weather episodes is not fully addressed, pioneering a methodology which simultaneously takes these two phenomena into account together will provide a novel modeling foundation towards resilience-enhanced interdependent critical infrastructure. Developing the proposed model facilitates planners to correctly understand the ICIs' behavior and make optimum resource allocation decisions. The solution sets determined by the proposed model are generally different from the set of solutions found by

the classic resilience-enhanced models which consider infrastructures separately. The potential deviation on outputs, however, saves metropolitan areas millions of dollars of unnecessary investments. It also provides the ICIs with higher capability for withstanding the extreme events, maintaining the operability in the higher stage, and relatively fast and less costly restoration. In this study, we have pioneered such an analytical foundation as a required extension to existing methodologies that provides a significant improvement on ICIs' performance, particularly when stressed or under attack.

REFERENCES

1. Lee, Hau L. "The triple-A supply-chain." Harvard business review 82, no. 10 (2004): 102-113.
2. Bruneau, Michel, et al. "A framework to quantitatively assess and enhance the seismic resilience of communities." Earthquake spectra 19.4 (2003): 733-752.
3. Ponomarov, Serhiy Y., and Mary C. Holcomb. "Understanding the concept of supply-chain resilience." The International Journal of Logistics Management 20, no. 1 (2009): 124-143.
4. Soni, Umang, and Vipul Jain. "Minimizing the vulnerabilities of supply-chain: A new framework for enhancing the resilience." In Industrial Engineering and Engineering Management (IEEM), 2011 IEEE International Conference on, pp. 933-939. IEEE, 2011.
5. Turnquist, Mark, and Eric Vugrin. "Design for resilience in infrastructure distribution networks." Environment Systems & Decisions 33, no. 1 (2013): 104-120.
6. Tomlin, Brian. "On the value of mitigation and contingency strategies for managing supply-chain disruption risks." Management Science 52.5 (2006): 639-657.
7. Jessup, Eric, et al. Development and analysis of a GIS-based statewide freight data flow network. No. WA-RD 730.1. Washington State Department of Transportation, 2009.
8. Tang, Christopher S. "Robust strategies for mitigating supply-chain disruptions." International Journal of Logistics: Research and Applications 9, no. 1 (2006): 33-45.
9. Ellwein LB, Gray P (1971) Solving fixed charge location-allocation problems with capacity and configuration constraints. AIIE T 3:290–299.
10. M.A. Cohen, M.L. Fisher, R. Jaikumar International manufacturing and distribution networks: a normative model framework.
11. Nozick, L., Turnquist, M., 1998a. Two-echelon inventory allocation and distribution center location analysis. In: Proceedings of Tristan III (Transportation Science Section of INFORMS), San Juan, Puerto Rico.

12. Nozick, L.K., Turnquist, M.A., 1998b. Integrating inventory impacts into a fixed charge model for locating distribution centers, Transportation Research Part E 31E (3), 173–186.

13. R.L. Church, C. ReVelle The maximal covering location problem Papers of Regional Science Association, 32 (1974), pp. 101–118.

14. Kuby, Michael, and Seow Lim. "The flow-refueling location problem for alternative-fuel vehicles." Socio-Economic Planning Sciences 39, no. 2 (2005): 125-145.

15. Hodgson, M. John. "A Flow-Capturing Location-Allocation Model." Geographical Analysis 22, no. 3 (1990): 270-279.

16. M. Kuby, S. Lim Location of alternative-fuel stations using the flow-refueling location model and dispersion of candidate sites on arcs Networks and Spatial Economics, 7 (2) (2007), pp. 129–152.

17. S. Lim, M. Kuby Heuristic algorithms for siting alternative-fuel stations using the flow refueling location model, European Journal of Operational Research, 204 (1) (2010), pp. 51–61.

18. Y.-W. Wang An optimal location choice model for recreation-oriented scooter recharge stations Transportation Research Part D: Transport and Environment, 12 (3) (2007), pp. 231–237.

19. Y.-W. Wang Locating battery exchange stations to serve tourism transport Transportation Research Part D: Transport and Environment, 13 (3) (2008), pp. 193–197.

20. ReVelle CS, Eiselt HA, Daskin MS (2008) A bibliography of some fundamental problem categories in discrete location science. Eur J Oper Res 184:817–848.

21. R. Current, C.S. ReVelle, J.L. Cohon The maximum covering/shortest path problem: a multiobjective network design and routing formulation Eur. J. Oper. Res., 21 (1985), pp. 189–199.

22. Lin, Zhenhong, Joan Ogden, Yueyue Fan, and Chien-Wei Chen. "The fuel-travel-back approach to hydrogen station siting." International journal of hydrogen energy 33, no. 12 (2008): 3096-3101.

23. Modeling Location decisions of retailers with an agent-based approach Francesco Ciari

24. An Agent-Based framework for modeling and solving location problems Giuseppe Bruno Andrea Genovese Antonino Sgalambro

25. Afshari, Hamid, et al. "Distribution-service Network Design: An Agent-based Approach." Procedia CIRP 17 (2014): 651-656.

26. Macal and North, 2010

27. An agent-based multi-objective optimization model for allocating public charging stations for electric vehicles Qi Han, Bauke de Vries and Geert Kanters

28. Layout of Gas Station Based on Multi-Agent Simulation

29. Shen, Weiming, and Douglas H. Norrie. "Agent-based systems for intelligent manufacturing: a state-of-the-art survey." Knowledge and information systems 1.2 (1999): 129-156.Sweda, T. and Klabjan, D. (2011) An Agent-Based Decision Support System for Electric Vehicle Charging Infrastructure Deployment